G E U S

Report file no.

14936

GRO-3

Organic geochemistry and thermal maturity of sediments in the GRO-3 well, Nuussuaq West Greenland

Bojesen-Koefoed, J.A., Christiansen, F.G., Nytoft, H.P. & Dalhoff, F.

GEUS
Copenhagen
17-04-1998

DANMARKS OG GRØNLANDS GEOLOGISKE UNDERSØGELSE RAPPORT 1997/143

Organic geochemistry and thermal maturity of sediments in the GRO#3 well, Nuussuaq, West Greenland

Jørgen Bojesen-Koefoed, Flemming G. Christiansen,
Hans Peter Nytoft and Finn Dalhoff

GEOLOGICAL SURVEY OF DENMARK AND GREENLAND
MINISTRY OF ENVIRONMENT AND ENERGY

GEUS

DANMARKS OG GRØNLANDS GEOLOGISKE UNDERSØGELSE RAPPORT 1997/143

Organic geochemistry and thermal maturity of sediments in the GRO#3 well, Nuussuaq, West Greenland

Jørgen Bojesen-Koefoed, Flemming G. Christiansen, Hans Peter Nytoft and Finn Dalhoff

GEOLOGICAL SURVEY OF DENMARK AND GREENLAND
MINISTRY OF ENVIRONMENT AND ENERGY

G E U S

Contents

Introduction

The GRO#3 well that was drilled on western Nuussuaq by grønArctic Energy Inc. (grønArctic) in the summer of 1996 is the first deep exploration well in the West Greenland onshore region. Information from this ~3 km deep well is therefore very import for the assessment of the exploration potential of the Nuussuaq basin. The present study of the organic geochemistry of the sediments in GRO#3 provides the best information so far on the thermal maturity gradient in the Nuussuaq basin, and the results are important for predicting the position of the oil window and the base of the oil preservation zone. Although previous studies have given some information on maturity gradients, data have been restricted to samples from outcrop sections that rarely exceed 500 m in height, with the thickest recorded continuous succession being the GANT#1 core (900 m of core). Due to these earlier restrictions in data availability, evaluation of GRO#3 maturity data has therefore been a key element in the EFP-95 project "Basin Modelling, Nuussuaq".

Furthermore, the many recorded oil seeps recognised recently and the oil-impregnated cores from previous drilling make organic geochemical studies of possible source rock intervals very important for correlation purposes (Christiansen *et al.* 1997; in press). The biomarker distributions of samples within the thick sedimentary succession penetrated in GRO#3 should therefore be compared with the biomarker fingerprinting of the seeping oils that has been well documented (Christiansen *et al.* 1996a; Bojesen-Koefoed *et al.* in press).

Geological setting

The West Greenland continental margin formed during the extensional opening of the Labrador Sea in Late Mesozoic – early Paleogene time. During this period a number sedimentary basins formed in the present Labrador Sea to the northern Baffin Bay region (e.g. Chalmers *et al.* 1993; Whittaker *et al.* 1997). The onshore part of these basins in West Greenland, the Nuussuaq Basin, extends from Disko in the south, across most of Nuussuaq, to Svartenhuk Halvø in the north (Fig. 1).

The Nuussuaq Basin is bounded against basement in the east by an extensional fault system, parts of which have been active several times during the late Mesozoic and early Cenozoic. Generally the basin is characterised by major N–S and NW–SE faults with E- and NE dipping fault blocks (Chalmers *et* al. in prep a,b). Major transpression in late Eocene or early Oligocene time, which is suggested to be related to movements along the NNE–SSW trending Ungava strike-slip fault system, has formed inversion anticlines and faults, e.g. along the Itilli valley (see Itilli Fault Zone on Fig. 1).

The sedimentary succession on Nuussuaq is in places 6 – 8 km thick (Christiansen *et al.*, 1995) of which the uppermost 2.5 km lower Cretaceous (Albian) to Paleocene succession is exposed. The sediments are typically overlain by 1.5–2 km of picritic hyaloclastites and continental flood basalts. The depositional pattern seems to be strongly structurally controlled, and especially the Kuugannguaq Fault zone is important. This major N–S trending normal fault zone that stretches from the Kuugannguaq valley on Disko, across the Vaigat and Nuussuaq (Fig. 1) acted as a major morphological feature throughout most of the Late Cretaceous – Paleocene. Deltaic deposition took place east of the fault (e.g. Pedersen & Pulvertaft, 1992), whereas, deposition in a major turbidite complex took place west of the fault (e.g. Dam & Sønderholm, 1994). Two phases of uplift in the Maastrichtian and Paleocene were associated with deep valley incision and subsequent infilling with possible reservoir sandstones (Kristensen & Dam 1997; Dam & Sønderholm in press; Dam *et al.* 1998).

GRO#3 was drilled in an area where the most obvious targets at the present stage of exploration are within the Campanian–Maastrichtian–lowermost Paleocene succession. This interval seems to contain several source rocks, potential reservoir turbidite sandstones enclosed in sealing marine mudstones, and potential mainly structural, traps within large rotated fault blocks. Although seismic data are scarce from the basin with the offshore Vaigat line being the only one in the vicinity of GRO#3, it is inferred that the well is at a position near the top of major fault block (more than 20 km west of the Kuuganguaq fault zone, less than 2 km east of the Gassø Fault zone) (Fig. 1). GRO#3 is situated at an up-dip position relative to GANE#1 that gave encouraging results when drilled in 1995.

Exploration by grønArctic and drilling of the GRO#3 well

In May 1995 grønArctic (with Platinova A/S as carried partner) was granted an exclusive exploration licence for a 1692 km^2 area covering western Nuussuaq. The license area was increased to 2355 km^2 in the spring of 1996, reduced to 988 km^2 by the end of 1996, and further reduced to 390 km^2 by the end of 1997. grønArctic began their exploration programme in July 1995 by drilling three slim-core holes, GANE#1, GANK#1 and GANT#1 (Christiansen *et al.* 1996b). The Geological Survey of Denmark and Greenland (GEUS) carried out the drill site geological description followed by a major sampling and analytical programme for grønArctic. A number of reports on the sedimentology, organic geochemistry and palynology of the cores and other samples from these holes have been made by GEUS (e.g. Dam 1996a,b,c; Christiansen *et al.* 1996c; Nøhr-Hansen 1997a).

grønArctic planned to drill two wells (GRO#1 and GRO#2) in 1996. The two targets were in the vicinity of GANK#1 and GANE#1, respectively, close to the Kuussuaq River (Fig. 1). After the drilling equipment was unloaded on the beach south-east of the Kuussuaq River delta, mobilization to the first planned site was suspended due to soft ground conditions and permafrost problems. An alternative well location, GRO#3, along a major structural complex (called PDZ = Principal Displacement Zone by grønArctic) adjacent to the Kuussuaq River delta (~ 1 km from the landing site) was then selected (Fig. 1). The well was spudded on August 3, 1996, completed by October 6, 1996, and reached a depth of 2996.2 m (Table 1).

grønArctic reported a number of sand intervals containing hydrocarbons and eight zones were tested. The drill stem test were performed by Alpine testers Ltd. All tests were negative and the well was abandoned. Mud logging services were provided by Sperry-Sun Mud Logging Services and geophysical well services including a full suite of logs, and a VSP (vertical seismic profiling) were provided by Schlumberger.

GEUS received well logs from GRO#3 in November 1996 and cuttings in February 1997. GEUS has subsequently made an independent evaluation of GRO#3 with focus on palynostratigraphy (Nøhr-Hansen 1997b), lithological interpretation and petrophysical evaluating including a correlation to nearby boreholes and exposures (Kristensen & Dam 1997), and organic geochemistry (present study).

Fig. 2 shows a simplified sedimentological and stratigraphic interpretation of GRO#3 with some geochemical data. The uppermost 300 m of the well penetrates Paleocene hyaloclastites whereas the remaining part is composed of mudstone and sandstone. The overall depositonal environment of this clastic system is interpreted as a marine slope with turbidite and debris flow deposits. The succession drilled in the GRO#3 well shows many similarities to the Itilli succession that is exposed ~15 km to the north-west (see Dam & Sønderholm 1994 for details). Diagenesis studies of the succession penetrated by the

GANT#1 well on northwestern Nuussuaq suggest that the most promising reservoir units should be found in the Paleocene part of the sedimentary sequence (Kirkegaard 1998).

The stratigraphic ages of the sediments from the base of the volcanics (~300m) down to 1485 m of the well have been reported as Late Selandian (Late Paleocene)–?Coniacian by Nøhr-Hansen (1997b) based on palynological dating. The samples from the deeper part is thermally altered to such a degree that dating is not possible. Assuming a stratigraphic thickness of the pre-Campanian succession comparable to the Umiivik-1 borehole on Svartenhuk Halvø area (see Nøhr-Hansen, 1997a; Dam *et al.* in press), the sediments at TD in GRO#3 may be Turonian or even older.

Analytical methods and organic geochemical programme

The analytical programme comprises standard organic geochemical analyses of a large number of drill cutting samples, in all cases of wet cuttings from plastic containers approx. 5 months after the well was terminated. Unfortunately cores or side-wall cores were not taken during the drilling programme. The organic geochemical analyses include:

Rock-Eval/TOC/TS screening analysis (n= 114). TOC analysis was carried out by means of a LECO IR212 induction furnace after elimination of carbonates from the samples by several stages of treatment with hot HCl. Rock-Eval pyrolysis was carried out roughly following the guidelines published by Espitalié *et al.* (1985). TS analysis was carried out by Haldor-Topsøe A/S by means of a LECO sulphur analyser.

Vitrinite reflectance analysis (n= 31).

Solvent extraction and group type fractionation (n=31). Solvent extraction was carried out by means of a Soxtech® apparatus, using dichloromethane+methanol (93+7 vol./vol.) as solvent. Aphaltenes were precipitated by addition of 40-fold excess of *n*-pentane. Maltene fractions were separated into saturated, aromatic and polar fractions using MPLC, following procedures modified from Radke *et al.* (1980).

GC and GC-MS biological marker analysis (n=31).

Results

Rock-Eval/TOC/TS screening

Screening data are tabulated in Table 2. Plots of Tmax vs. HI, and TOC vs. S2 are shown in Fig. 3 and Fig 4, and plots of screening data against depth are shown in Fig 5.

Total organic carbon contents (TOC) of the mudstones vary from 1.15% to 6.55% (average: 4.46%) and show little systematic variation with depth (Fig. 2). However, in the uppermost (Paleocene) part of the succession (320m - 510m), TOC tends to be slightly lower than in the deeper part.

Total sulphur contents (TS) are generally high through the entire succession, covering the range from 0.52% to 3.83% (average 1.83%). A plot of TOC vs TS is shown in Fig. 6. Many of the thicker mudstone intervals show a distinct "sulphuring-upwards" trend (Fig. 2). In some of the mudstone units this upward increase in sulphur is associated with a minor increase in TOC.

S1 is generally low, never attaining values greater the 1.14 mg/g. Maximum values are found in the interval 1100-1500m, and at greater depths a fairly regular decrease is observed, until constant values close to zero are attained at depths greater than ~2200m. S2 is very variable, ranging from 8.08 mg/g to 0.04 mg/g (average 2.06 mg/g). Values greater than 2.0 mg/g are restricted to the upper part of the succession, i.e. to depths shallower than ~1700m. In this interval considerable scatter is present, but in deeper parts of the succession a regular decrease is observed until largely constant values close to zero are attained at depths greater than ~2200m. Hydrogen Index (HI) varies from 217 to 4 (average 50). Although some scatter is present in the upper part of the succession (i.e. depths shallower than ~1400m) a fairly regular decrease in HI with depth is observed.

Tmax ranges from 431° C to 575° C and shows a regularly increasing, slightly sigmoidal trend with depth. Vitrinite reflectance (R_o) ranges from 0.71% to 2.63%, and shows a regularly increasing trend with depth.

Solvent Extraction and Gas Chromatography

Solvent extraction and group type fractionation data are listed in Table 3. Parameters calculated from gas chromatographic data are listed in Table 4, and individual chromatograms are shown in Fig. 9.

Solvent extract yields are generally low to moderate, less than 89 mg/g organic carbon. At depths greater than ~1400m, very low values are noted, 1–21 mg/g, and in a few samples the amount of extract recovered was too small even to be determined. Hence, solvent extraction and GC/GC-MS data from this part of the drilled succession should be used with caution. Although some scatter is present, an overall decreasing trend of extract yield with

depth is noted. Asphaltene contents are somewhat variable, ranging from 46% to 19% of the total extract, and an overall decrease in the proportion of asphaltenes with depth is noted. Maltene fraction compositions are dominated by polar compounds, which constitute 43% to 88%. Hydrocarbon fractions are, except for a few samples, dominated by saturated compounds, with sat/aro ratios in the range 1 to 7. Excluding the part of the drilled succession deeper than ~1400m, sat/aro ratios show an overall increasing trend with depth.

Gas chromatograms of saturated solvent extract fractions show significant changes in *n*-alkane distributions with depth. In the upper part of the drilled succession, i.e. 320–510 m, heavy-end skewed distributions, with pristane/nC_{17}>1 and CPI >1 are observed. In the deeper part of the succession, *n*-alkane distributions grow increasingly light-end skewed, as pristane/nC_{17} decreases to values <1, and CPI approaches 1. At depths greater than ~1500m *n*-alkane distributions are somewhat variable, and rather poor signal-to-noise ratios are noted in some of the chromatograms. A facies-change may be indicated by a shift in pr/ph ratios to values close to 1, but light-end truncation, odd-number predominance, and abundance of unknowns are also observed in a number of these deeper samples. In particular data from the four deepest samples are doubtful.

Biological Marker data

The concentration of biological marker compounds generally decreases with depth, leading to poor signal-to-noise ratios, and accordingly, to limited utility of data from samples collected deeper than ~1500m. Most variation can be related to the marked maturity-increase with depth, but a few facies-related features are of note, and will be discussed below.

At depths shallower than ~1500m, triterpane biological markers are dominated by pentacyclic components of the hopane series, with variable proportions of oleanane, taraxastane, and compounds of the lupane series (lupane, norlupane, bisnorlupanes) (see Bojesen-Koefoed *et al.* 1997; Bojesen-Koefoed *et al.* in press). In the upper part of the succession, tricyclic triterpanes are present in very low proportions only, but below ~1000m increasing proportions with depth are noted. A C_{24} tetracyclic terpane is present in all samples, and shows a depth-trend largely parallel to that of the tricyclic triterpanes. Regular steranes are clearly dominated by C_{29} steranes, with S27/S29 ratios in the range 0.1–0.8 (average 0.3), and C_{30} steranes are not detected. Possibly, a tendency for increasing S27/S29 ratios over the interval 1000-1500m. Variable proportions of 28,30 bisnorhopane are detected in six samples (340m, 510m, 1170m, 1180m, 1230m, 1250m). In addition, C_{28} ring-A methylated steranes are present in two samples (340m, 510m), together with extended 28-norhopanes (Bojesen-Koefoed *et al.* in press; Nytoft *et al.* in prep.).

A facies-change is noted in the interval 1500-2300m, indicated by S27/S29 ratios >1, presence of C_{30} steranes, and pr/ph ratios close to 1. However, data from the part of the succession deeper than ~1500m are characterised by poor signal to noise-ratios, and in particular data from the four deepest samples are doubtful.

Discussion and conclusions

Petroleum Source Rock Potential

The source rock potential of the mudstones of the penetrated succession shows a strong dependence on the depth-related maturity level discussed below. In general, TOC is high, but the pyrolysis yield is poor to fair - only few samples may be rated good. The kerogen may be roughly classified as type III, but the content of inert/non-pyrolysable organic matter is evidently very high (Figs 3 & 4). The samples analysed represent the average compositions of rock units which are probably not homogeneous with respect to petroleum source potential. Hence, the Hydrogen Indices stated may not be representative of the actual source potential, since a significant proportion of the organic matter (perhaps amounting to several percent TOC) is unlikely to contribute to the potential, and may thus be left out of the HI calculation.

Samples from the Paleocene part of the succession (~320–510m) plot close to the "normal marine" line in the TOC vs TS plot shown in Fig. 6, whereas samples from the deeper part of the succession plot to the right of the trendline, indicating increased proportions of TOC relative to TS. This observation can be explained by the presence of excess proportions of inert organic matter in the deeper samples, corresponding to the higher average TOC yielded by these samples, which was noted earlier. Hence, the apparent "less-marine" TS/TOC ratios observed in these deeper samples are artefacts, produced by the presence of organic matter, which due an initially inert nature has not taken part in the microbial processes leading to the correlation of TS and TOC often observed in normal marine sediments (e.g. Berner & Raiswell 1984).

Thermal Maturity

A well developed depth-dependant maturity-trend is observed throughout the penetrated succession. This is consistently indicated by several types of data, including Rock-Eval screening (principally Tmax, but also S1, S2, and HI), vitrinite reflectance (R_o), and biological marker parameters such as Ts/(Ts+Tm), moretane/hopane, and C_{29} regular sterane $\alpha\beta\beta/(\alpha\beta\beta+\alpha\alpha\alpha)$ ratios (figs 5 & 11). Other traditional biological marker maturity indicators such as homohopane 22S/(22S+22R) and regular sterane 20S/(20S+20R) epimerization ratios have reached their equilibrium values in the uppermost part of the penetrated succession, and do not show change with depth. A good correlation of Tmax and R_o is observed (fig. 7). The "oil window" is defined as the maturity interval yielding vitrinite reflectances in the range 0.50% – 1.20%, which according to the observed correlation corresponds to values of Tmax in the range 418°–467°. By comparison with published values, a

Tmax-value of 418° at the top of the oil window is approximately 10° to low, whereas a value of 467° at the base of the oil window is in perfect agreement with literature data (e.g. Bordenave *et al.* 1993).

The vitrinite reflectance trend recorded in the GRO#3 well is remarkably regular and bears no witness of any kind of anomalies caused by intrusions, hydrothermal activity or changes in maturity gradients across possible unconformities. This undisturbed maturity trend seems to be the result of a simple subsidence history only.

Based on the vitrinite reflectance trend recorded in the GRO#3 well, the position of the oil window, as defined by thermal maturities in the range from R_o=0.50 % to R_o=1.20 %, can be determined as the interval from approximately 260 m above the present day surface at the drilling site, to approximately 1300 m below the surface (fig. 8). This result is in perfect agreement with indications from other data. Hence, based on the S1- and S2-trends, it is estimated that the oil window is restricted to the interval from the base of the basalts (~300m) to ~1500m. Below ~1500m, S1 and S2 both decrease rapidly, indicating that generation still took place here during deepest subsidence, however, with a predominance of more gaseous products which have not been retained in the samples to be detected as the S1 parameter. This interpretation is supported by extraction yields, which show a strong decline at depths greater than ~1400m.

By extrapolation of R_o data, the thickness of the "missing", presumably mainly volcanic, succession can be estimated at ~1890m. This corresponds fairly well to the maximum height of the mountains in the hinterlands (fig. 8) and gives important constraints on the magnitude of uplift and erosion of the area.

The base of the oil preservation zone is estimated to ~2200m (corresponding to a vitrinite reflectance value of approximately 1.9%), at which depth both S1, S2, and extract yields are largely equal to zero. Furthermore, below this depth various biological marker data seem spurious, probably influenced by the presence of caved material and random contamination from unknown sources. This estimated oil preservation limit is in agreement with previous estimates based on shallower boreholes and surface data (Christiansen *et al.* 1996c).

Based on palynological, sedimentological and petrophysical log data a consistent correlation between the 497m–565m section in the GANE#1 well and the 320m–370m section in the GRO#3 well can be established (Nøhr-Hansen 1997b; Kristensen & Dam 1997). Screening data do not reveal any significant maturity difference between these intervals in GRO#3 and GANE#1. However, biological marker data, principally Ts/(Ts+Tm), Tm/(Tm+17β), and sterane epimerisation ratios systematically show the succession drilled in the GRO#3 well to be slightly more mature than the equivalent succession in GANE#1, despite a greater depth (relative to sea level) in the latter. It is possible that the geothermal gradient (heat flow) was slighter higher towards the west (GRO#3 is situated ~4 km west of GANE#1), thereby causing comparable higher thermal maturities in the GRO#3 well. These observations on the thermal maturity may also have important structural implica-

tions, as they may suggest that the structures were formed after the main phase of subsidence and thermal maturation and possibly also primary migration. The formation of some of these structures may be related to transpression in the Eocene or Oligocene.

Organic facies

With minor variations (see below), the sediments analysed in the upper portion of the well, i.e. the interval 320–510 m, show biological marker distributions closely resembling that of the Marraat oil type (Christiansen *et al.* 1996a, Bojesen-Koefoed *et al.* in press). Although correlation in a strict sense cannot be established, the similarities are obvious, and all samples represent sedimentary environments receiving large proportions of terrigenous organic matter. Given the variability of the chemical signatures of the rocks analysed in the GRO#3 well, it is indeed conceivable that the Marraat oil type was generated from source rocks equivalent to the sediments present in the upper part of the GRO#3 well. This interpretation is primary based on the high concentrations of distinct angiosperm derived biomarkers.

As previously noted, the two samples collected at 340m and 510m contain certain components which are not observed in the Marraat oil type. The presence of ring-A methylated steranes and extended 28-norhopanes in the 340m and 510m is remarkable, since these features are characteristics of the Eqalulik oil-type analysed in the GANE#1 and GANK#1 cores and in surface samples of this oil type mixed with other oil types (Bojesen-Koefoed *et al.* in press). These compounds have not previously been detected in sediment samples from the Nuussuaq basin. However, despite the presence of these unusual components, the sediments analysed in the GRO#3 well are obviously not the sources of the Eqalulik oil type, since the biological marker distribution in general does not correspond to that of the Eqalulik oil type.

Despite the poor data quality in samples from the deeper part of the succession, several parameters, including pr/ph and sterane data, point to a comparatively more marine nature of the sediments samples collected in the interval 1500-2300m. The four deepest samples (2510m (2 samples), 2875m, 2950m) show a number of anomalous features which are not conformable with high thermal maturity. Furthermore the extract recovery from these samples is extremely low, increasing the risk of contamination. Hence, data from these samples are discounted.

Acknowledgements

The present study (analyses and interpretation) was financially supported by the EFP-95 Project "Basin modelling, Nuussuaq". John Boserup prepared the sample material, while Ditte Kiel-Dühring, Carsten Guvad and Lisbeth L. Nielsen made the laboratory analyses. Hanne B. Sørensen and Jannie S. Larsen helped with the technical preparation of the report.

References

Berner, R. A. & Raiswell, R. 1984. C/S method for distinguishing freshwater from marine sedimentary rocks. Geology 12, 365-368.

Bojesen-Koefoed, J. A., Christiansen, F. G., Nytoft, H. P. & Pedersen, A. K. 1997: Seep data from onshore West Greenland. Danmarks og Grønlands Geologiske Undersøgelse Rapport **1997/34**, 7 pp., 7 figs, 8 tables.

Bojesen-Koefoed, J. A., Christiansen, F. G., Nytoft, H. P. & Pedersen, A. K. in press: Oil seepage onshore West Greenland: evidence of multiple source rocks and oil mixing. In: A. M. Spencer (ed.) Petroleum Geology of NW-Europe, Proceedings of the 5th Conference

Bordenave, M. L., Espitalié, J., Leplat, P., Oudin, J. L. & Vandenbroucke, M. 1993: Screening techniques for Source Rock Evaluation. In: Bordenave, M. L. (ed.) Applied Petroleum Geochemistry, Éditions Technip, Paris, 219–278

Chalmers, J. A., Pulvertaft, T. C. R., Christiansen, F. G., Larsen, H. C., Laursen, K. H. and Ottesen, T. 1993: The southern West Greenland continental margin: rifting history, basin development, and petroleum potential. In: Parker, J. R. (ed.) Petroleum Geology of Northwest Europe: Proceedings of the 4th Conference, 915–931.

Chalmers, J. A., Pulvertaft, T. C. R. & Marcussen, C. in prep a: New structure maps over the Nuussuaq Basin, central West Greenland. Submitted to Geology of Greenland Survey Bulletin

Chalmers, J. A., Marcussen, C., Pedersen, A. K. & Pulvertaft, T. C. R. in prep b: New light on the structure of the petroliferous Nuussuaq Basin, central West Greenland. To be submitted to Marine and Petroleum Geology

Christiansen, F. G., Marcussen, C. and Chalmers, J. A. 1995: Geophysical and petroleum geological activities in the Nuussuaq–Svartenhuk Halvø Area 1994 – promising results for an onshore exploration potential. Rapport Grønlands Geologiske Undersøgelse **165**, 32–41.

Christiansen, F. G., Bojesen-Koefoed, J., Dam, G., Nytoft, H. P., Larsen, L. M., Pedersen, A. K. and Pulvertaft, T. C. R. 1996a: The Marraat oil discovery on Nuussuaq, West Greenland: evidence for a latest Cretaceous–earliest Tertiary oil prone source rock in the Labrador Sea–Melville Bay region. Bulletin of Canadian Petroleum Geology **44**, 39–54.

Christiansen, F. G., Bate, K. J., Dam, G., Marcussen, C. & Pulvertaft, T. C. R. 1996b: Continued geophysical and petroleum geological activities in West Greenland in 1995 and start

of an onshore exploration programme. Bulletin Grønlands Geologiske Undersøgelse **172**, 15–21.

Christiansen, F. G., Bojesen-Koefoed, J. A., Nytoft H. P. & Laier, T. 1996c: Organic geochemistry of sediments, oils and gases in the GANE#1, GANT#1 and GANK#1 wells, Nuussuaq, West Greenland. Danmarks og Grønlands Geologiske Undersøgelse Rapport **1996/23**, 35pp + app.

Christiansen, F. G., Boesen, A., Dalhoff, F., Pedersen, A. K., Pedersen, G. K., Riisager, P. and Zinck-Jørgensen, K. 1997: Petroleum geological activities onshore West Greenland in 1996, and drilling of a deep exploration well. Geology of Greenland Survey Bulletin **176**, 17–23.

Christiansen, F. G., Boesen, A., Bojesen-Koefoed, J., Dalhoff, F., Dam, G., Neuhoff, P., Pedersen, A. K., Pedersen, G. K., Stannius, L. S. & Zinck-Jørgensen, K. in press: Petroleum geological activities onshore West Greenland in 1997. Geology of Greenland Survey Bulletin

Dam, G. 1996a: Sedimentology of the GANE#1 and GANE#1A cores drilled by grønArctic energy inc., Eqalulik, Nuussuaq, West Greenland. Danmarks og Grønlands Geologiske Undersøgelse Rapport **1996/82**, 18 pp., 2 figs, 2 tables.

Dam, G. 1996b: Sedimentology of the GANK#1 and GANK#1A cores drilled by grønArctic energy inc., Kuussuaq, Nuussuaq, West Greenland. Danmarks og Grønlands Geologiske Undersøgelse Rapport **1996/83**, 14 pp., 2 figs, 2 tables.

Dam, G. 1996c: Sedimentology of the GANT#1 core drilled by grønArctic energy inc., Tunorssuaq, Nuussuaq, West Greenland. Danmarks og Grønlands Geologiske Undersøgelse Rapport **1996/96**, 18 pp., 2 figs, 1 appendix (60 pp).

Dam, G. & Sønderholm, M. 1994: Lowstand slope channels of the Itilli succession (Maastrichtian–Lower Paleocene), Nuussuaq, West Greenland. Sedimentary Geology **94**, 49–71.

Dam, G. & Sønderholm, M. in press: Sedimentological evolution of a fault-controlled incised valley system, Lower Paleocene Quikavsak Member, Nuussuaq, West Greenland. In: Shanley, K. W. and McCabe, P. J. (eds) Relative role of eustacy, climate, and tectonism in continental rocks. Society of Economic Paleontologists and Mineralogists, Special Publication, **59**,

Dam, G., Larsen, M. & Sønderholm, M. 1998: Sedimentary response to mantle plumes: implications from the Paleocene onshore West and East Greenland. Geology **26**, 207-210.

Dam, G., Nøhr-Hansen, H., Christiansen, F. G., Bojesen-Koefoed, J. A. & Laier, T. in press: The oldest marine Cretaceous sediments in West Greenland (Umiivik-1, Svartenhuk

Halvø) - record of the Cenomanian–Turonian anoxic event? Geology of Greenland Survey Bulletin

Espitalié, J., Deroo, G. & Marquis, F., 1985: La pyrolyse Rock-Eval et ses applications - Première partie. Revue de l'Institut Français du Pétrole **40**, 563-579.

Kristensen; L. & Dam, G. 1997: Lithological and petrophysical evaluation of GRO#3 well, Nuussuaq, West Greenland. Danmarks og Grønlands Geologiske Undersøgelse Rapport **1997/156**, 30 pp.

Kirkegaard, T. 1998. Diagenesis and reservoir studies of Cretaceous–Lower Tertiary sandstones: the GANT#1 well, western Nuussuaq, central West Greenland. Danmarks og Grønlands Geologiske Undersøgelse Rapport 1998/7, 53 pp.

Nytoft, H. P., Bojesen-Koefoed, J. A. & Christiansen, F. G. in prep: 28-norhopanes in sediments and petroleum. Maturity parameters based on C29-C30 28-norhopanes. To be submitted to Organic Geochemistry

Nøhr-Hansen, H. 1997a: Palynology of the boreholes GANE#1, GANK#1 ant GANT#1, Nuussuaq, West Greenland. Danmarks og Grønlands Geologiske Undersøgelse Rapport **1997/89,** 23 pp., 6 figs, 6 plates.

Nøhr-Hansen, H. 1997b: Palynology of the GRO#3 well, Nuussuaq, West Greenland. Danmarks og Grønlands Geologiske Undersøgelse Rapport **1997/151**, 19 pp., 3 figs, 1 plate, 1 enclosure.

Pedersen, G. K. & Pulvertaft, T. C. R. 1992: The nonmarine Cretaceous of the West Greenland basin, onshore West Greenland. Cretaceous Research **28,** 263–272.

Radke, M., Willsch, H. & Welte, D. H., 1980. Preparative hydrocarbon group type determination by automated medium pressure liquid chromatography. Analytical Chemistry **52**, 406-411.

Whittaker, R. C., Hamann, N. E. & Pulvertaft, T. C. R. 1997. A new frontier province offshore Northwest Greenland: structure, basin development, and petroleum potential of the Melville Bay area. AAPG Bulletin 81, 978-998.

Figures

Tables

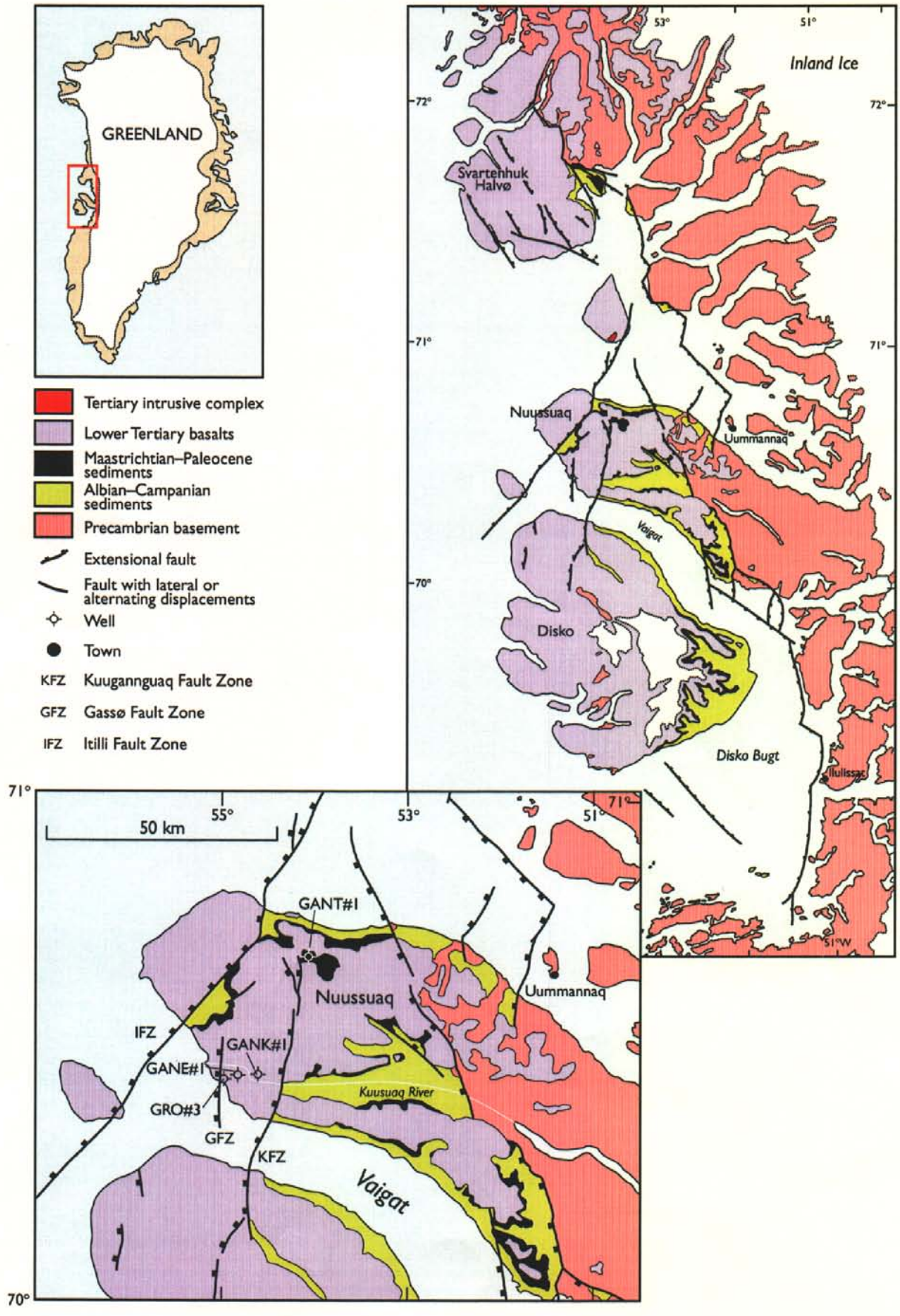
GREENLAND
Tertiary intrusive complex
Lower Tertiary basalts
Maastrichtian–Paleocene sediments
Albian–Campanian sediments
Precambrian basement
Extensional fault
Fault with lateral or alternating displacements
Well
Town
KFZ Kuugannguaq Fault Zone
GFZ Gassø Fault Zone
IFZ Itilli Fault Zone
Inland Ice
Svartenhuk Halvø
Nuussuaq
Uummannaq
Vaigat
Disko
Disko Bugt
Ilulissat
50 km
GANT#1
GANK#1
GANE#1
GRO#3
IFZ
GFZ
KFZ
Kuusuaq River
72°
71°
70°
53°
51°
55°

Fig. 1

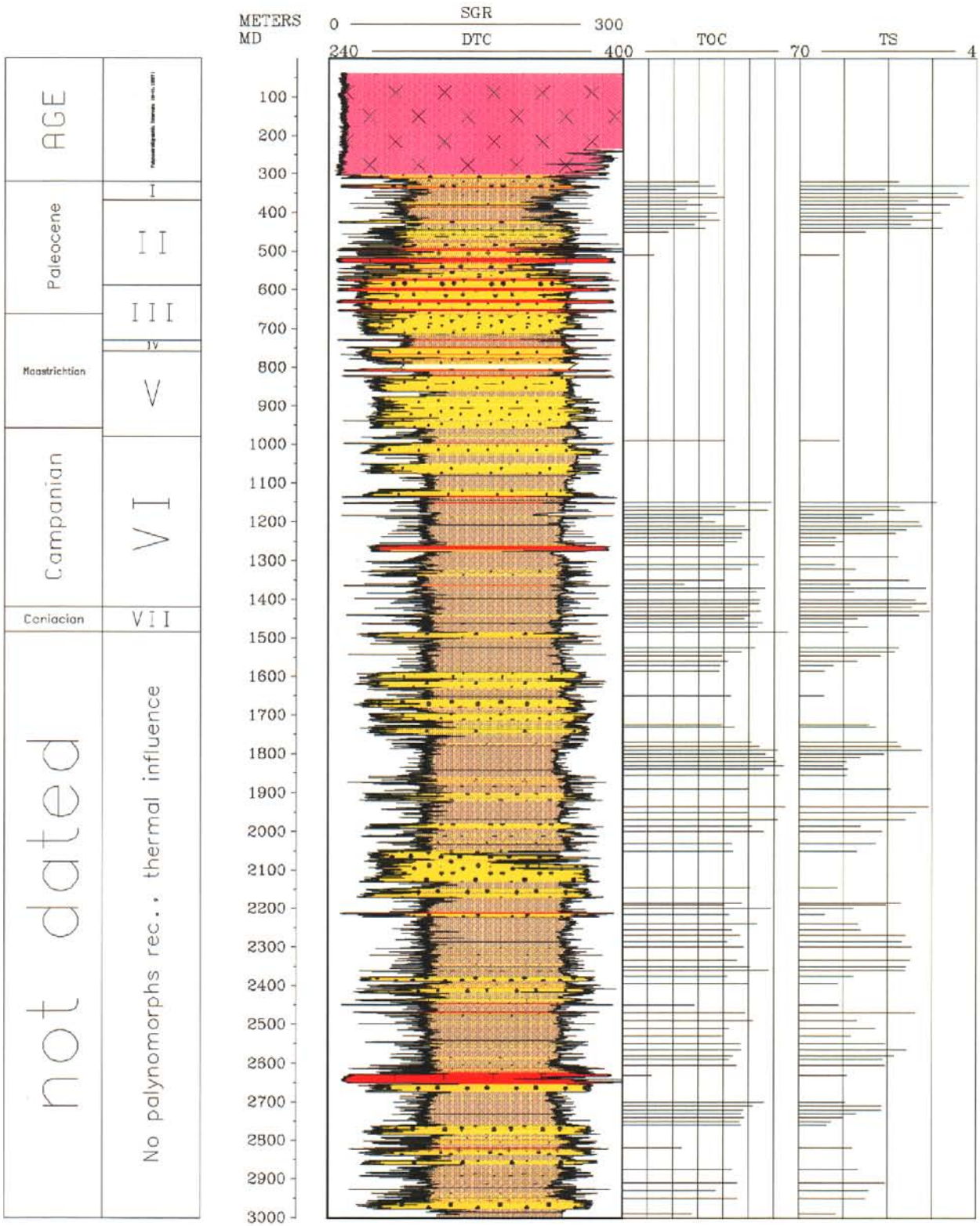

Log Curves	
SGR	Spectometry Gamma Ray
DTC	Sonic Log
TOC	Total Organic Carbon
TS	Total Sulphur

Legend
Hyaloclastites
Sandstone
Heterolith
Igneous intrusive
Mudstone
Tuff mixed with shale

Fig. 2

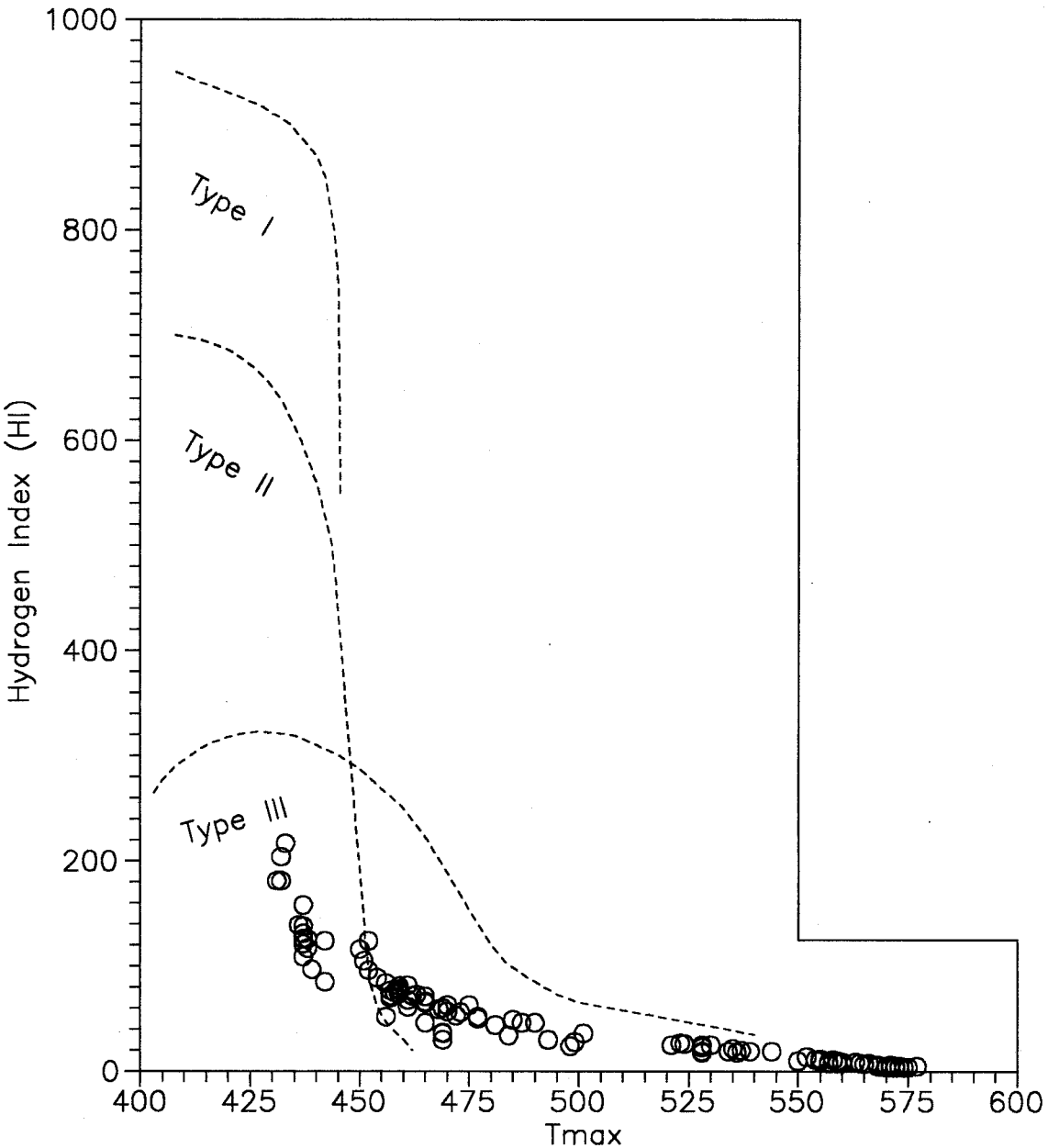
1000
800
600
400
200
0
Hydrogen Index (HI)
Type I
Type II
Type III
400
425
450
475
500
525
550
575
600
Tmax

Fig. 3

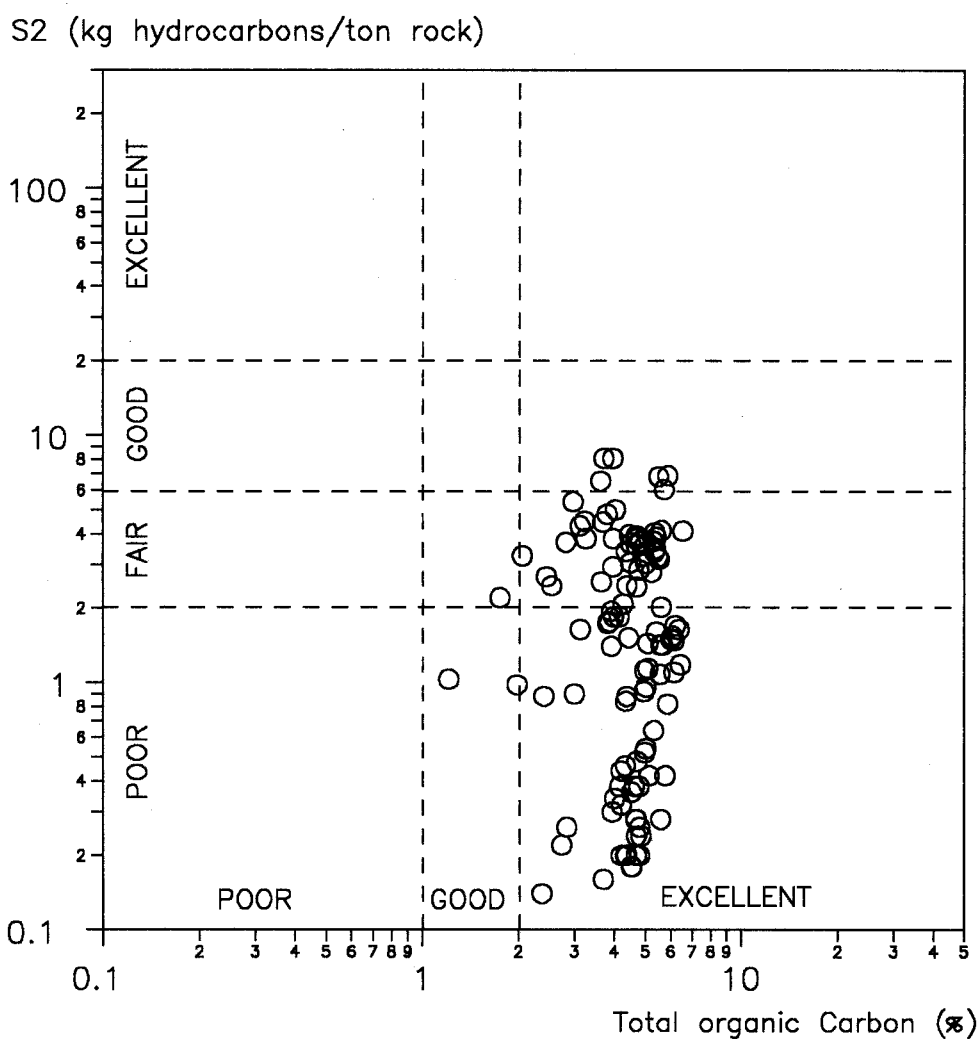
S2 (kg hydrocarbons/ton rock)
100
10
1
0.1
EXCELLENT
GOOD
FAIR
POOR
POOR
GOOD
EXCELLENT
0.1
1
10
Total organic Carbon (%)

Fig. 4

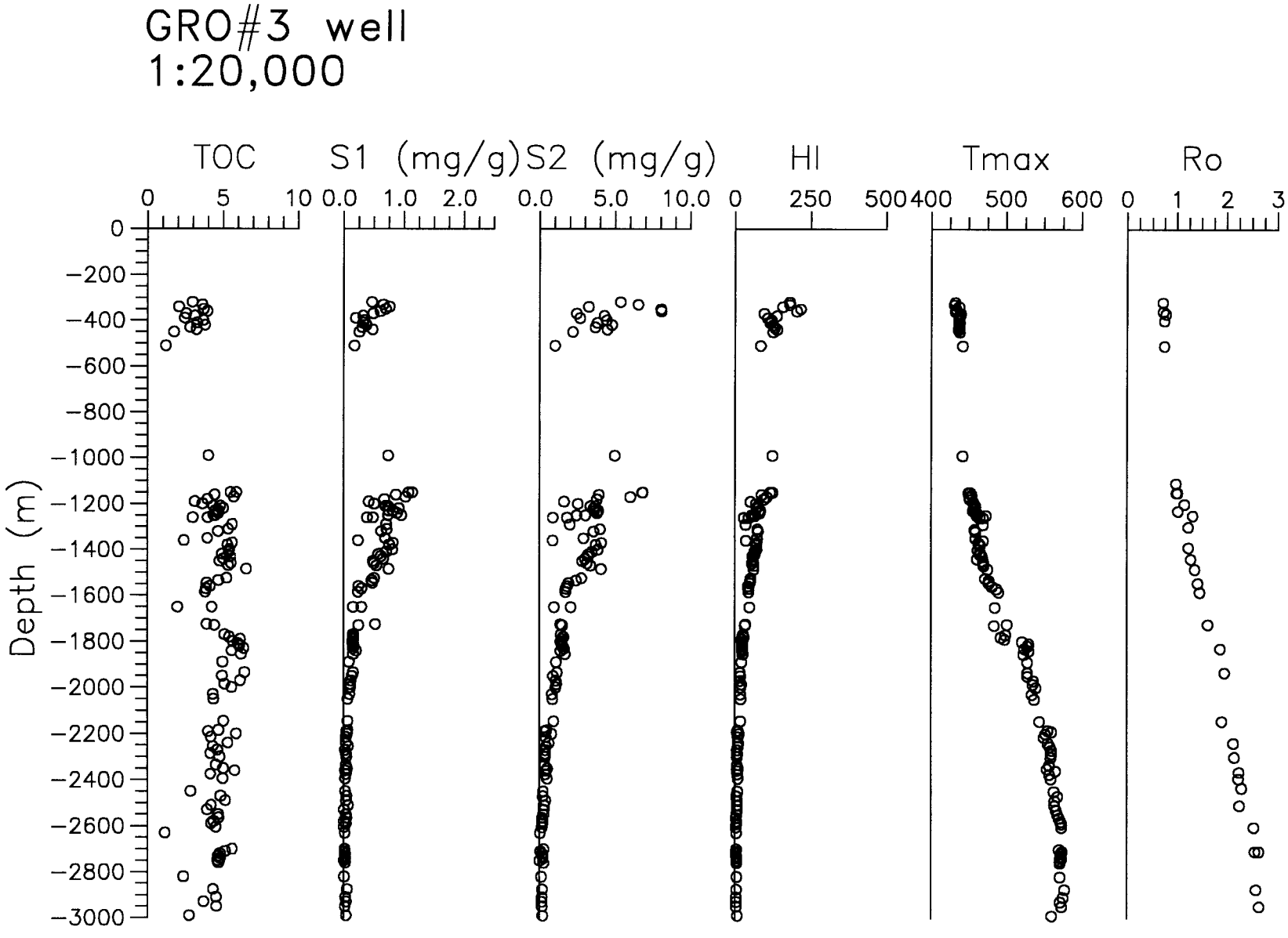
GRO#3 well
1:20,000
TOC
S1 (mg/g)
S2 (mg/g)
HI
Tmax
Ro
0
5
10
0.0
1.0
2.0
0.0
5.0
10.0
0
250
500
400
500
600
0
1
2
3
Depth (m)
0
−200
−400
−600
−800
−1000
−1200
−1400
−1600
−1800
−2000
−2200
−2400
−2600
−2800
−3000

Fig. 5

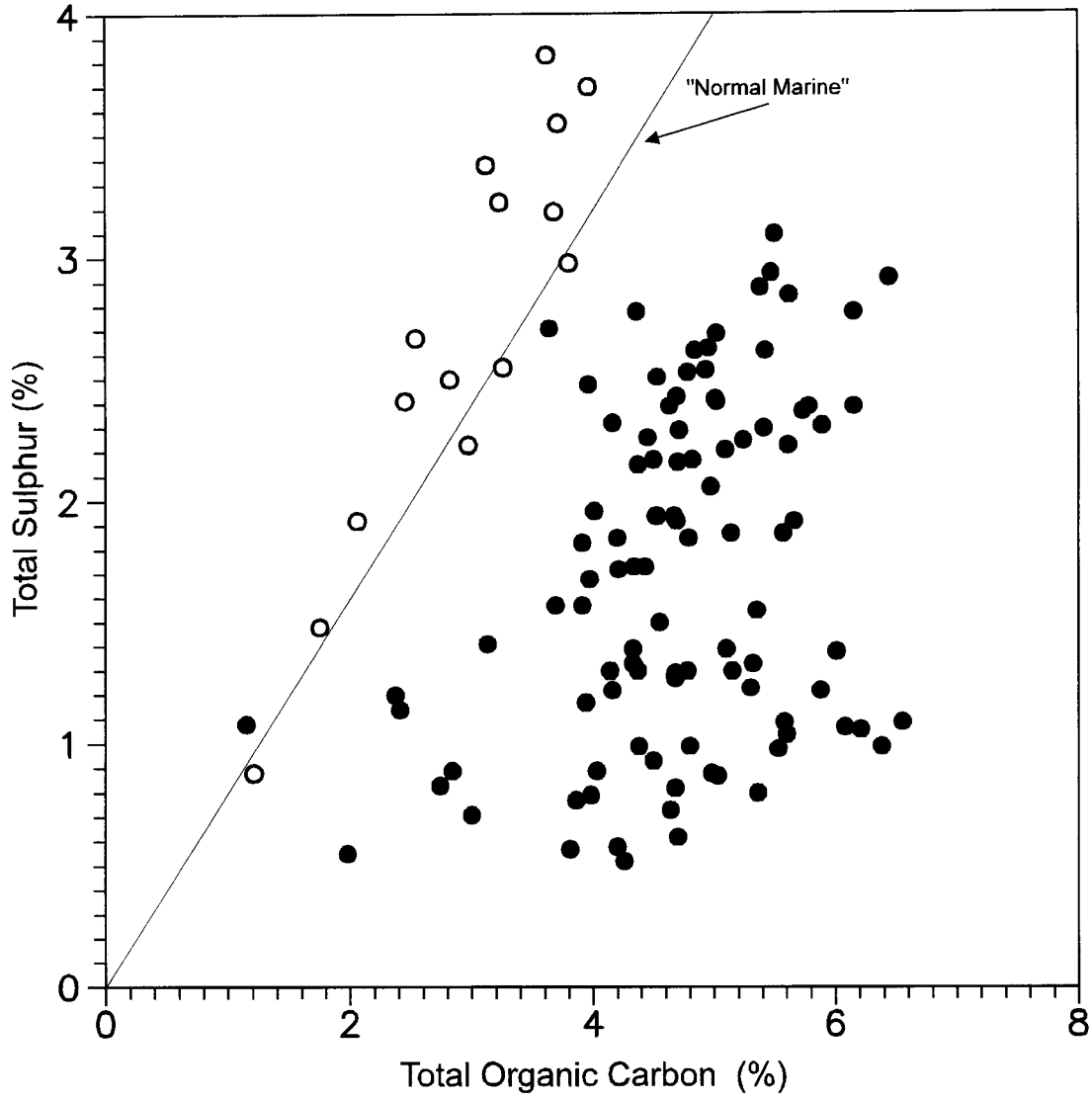
"Normal Marine"
Total Sulphur (%)
Total Organic Carbon (%)
0
1
2
3
4
0
2
4
6
8

Fig. 6

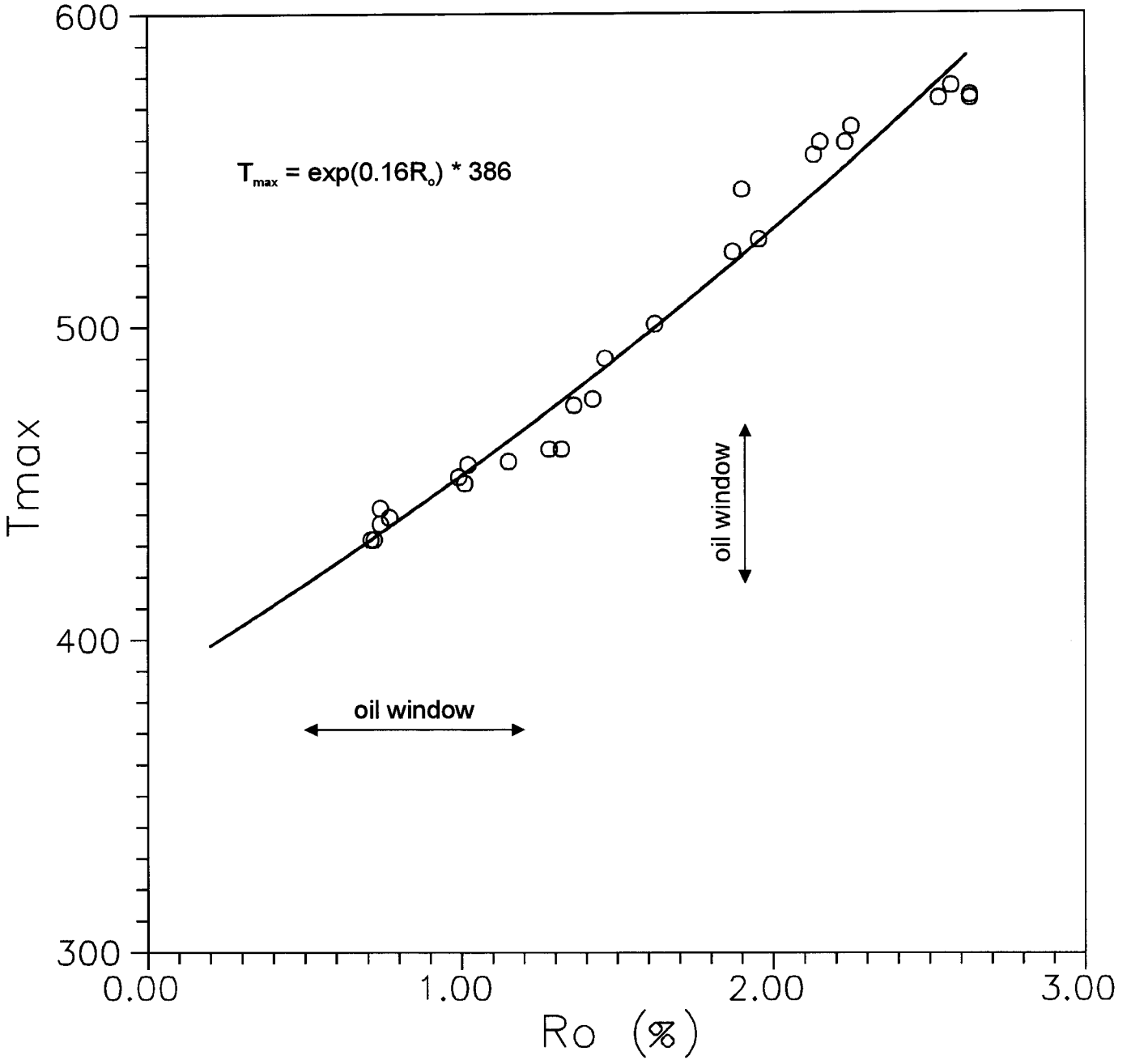
600
500
400
300
Tmax
0.00
1.00
2.00
3.00
Ro (%)
$T_{max} = exp(0.16R_o) * 386$
oil window
oil window

Fig. 7

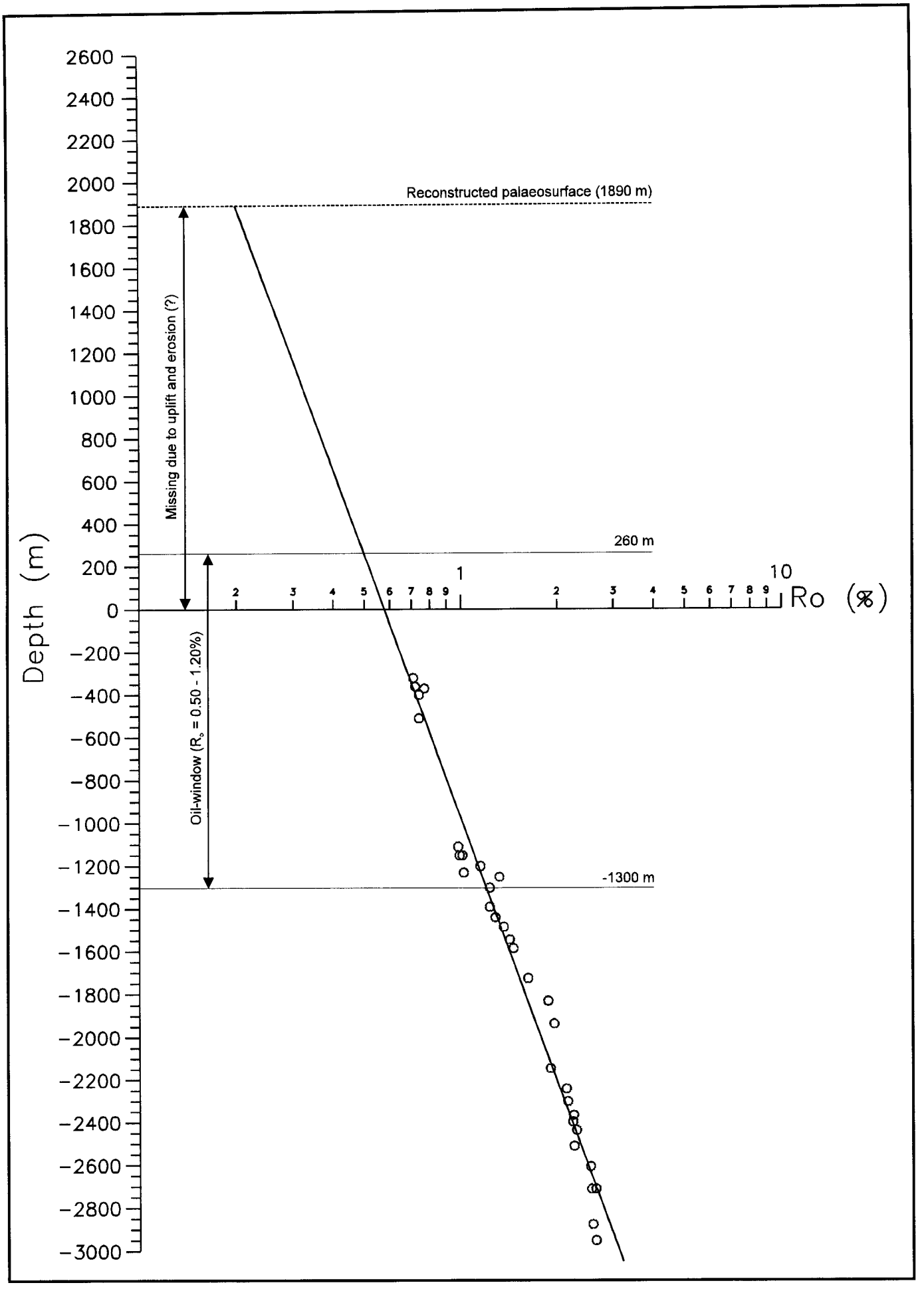
Depth (m)
2600
2400
2200
2000
1800
1600
1400
1200
1000
800
600
400
200
0
−200
−400
−600
−800
−1000
−1200
−1400
−1600
−1800
−2000
−2200
−2400
−2600
−2800
−3000
Reconstructed palaeosurface (1890 m)
Missing due to uplift and erosion (?)
260 m
Oil-window (R_o = 0.50 - 1.20%)
-1300 m
1
2
3
4
5
6
7
8
9
10
Ro (%)

Fig. 8

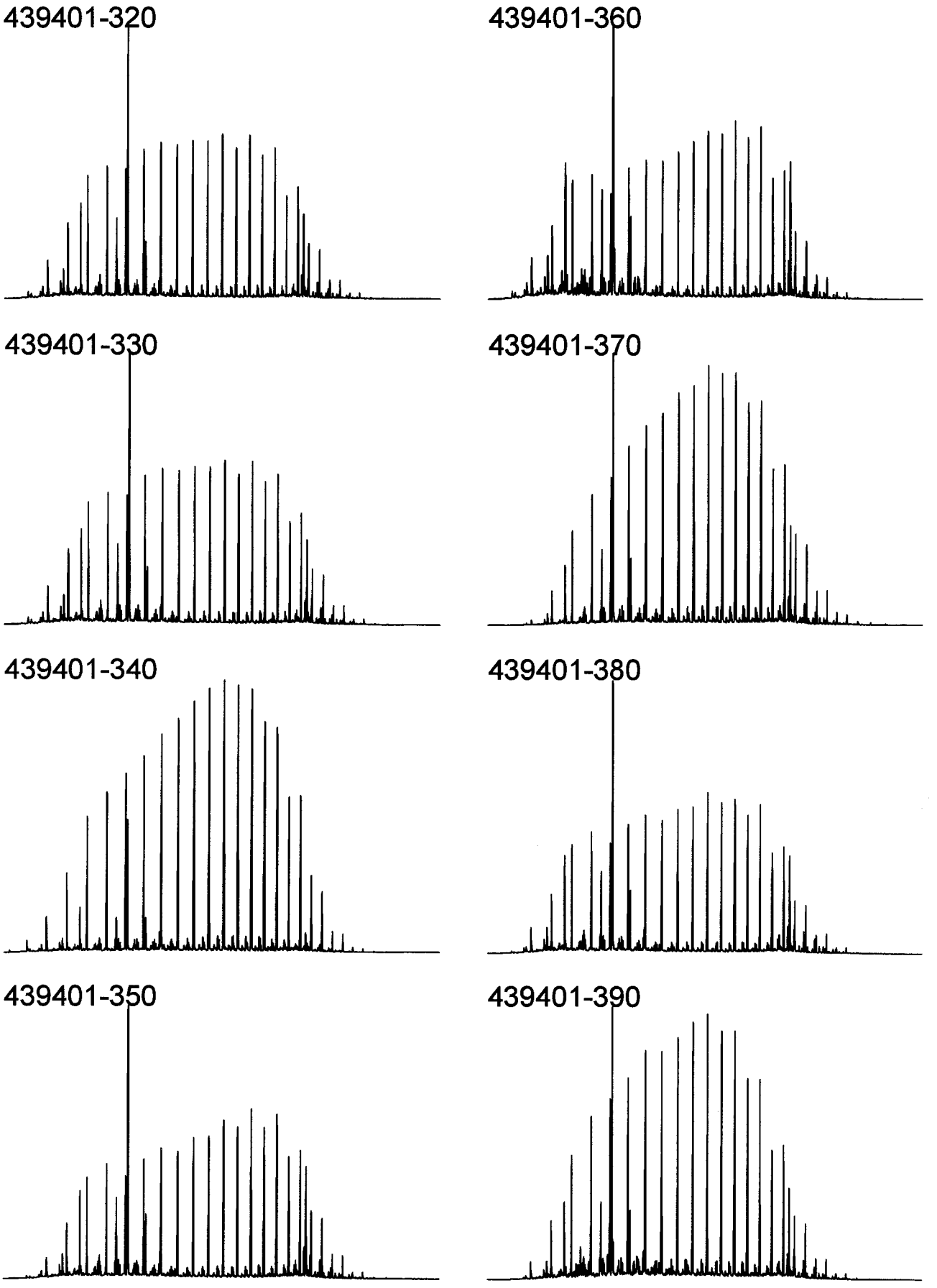
439401-320
439401-360
439401-330
439401-370
439401-340
439401-380
439401-350
439401-390

Fig. 9

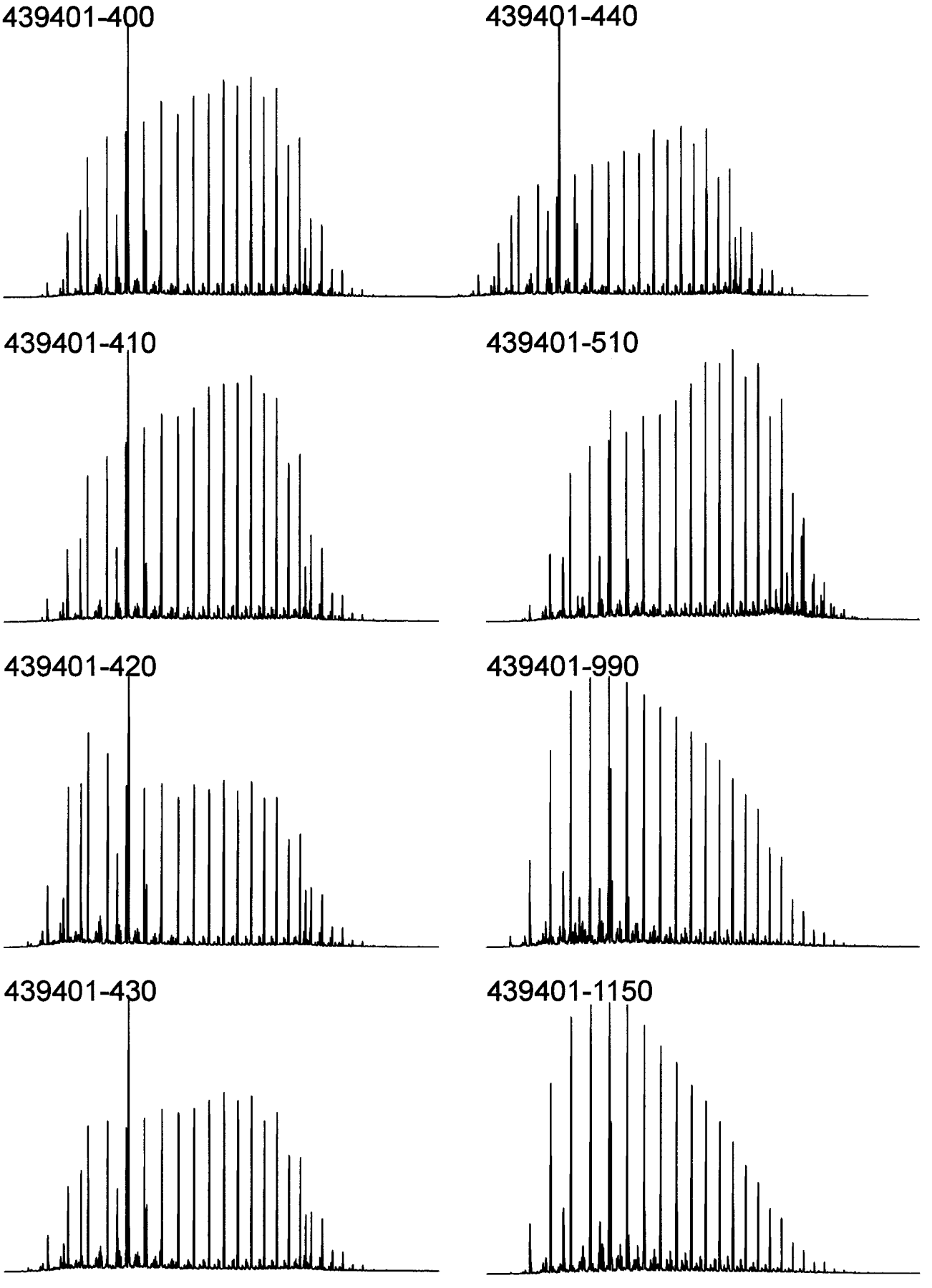

Fig. 9 continued

439401-1170

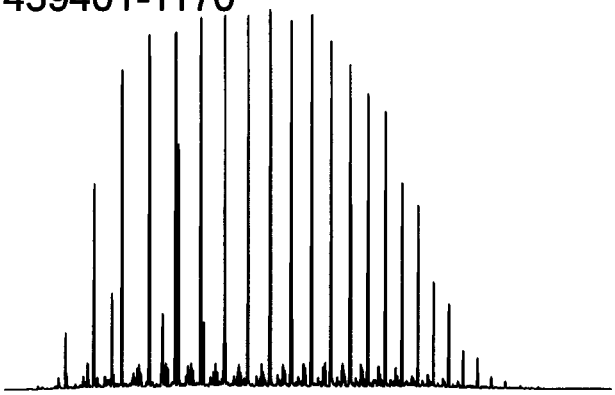

439401-1370

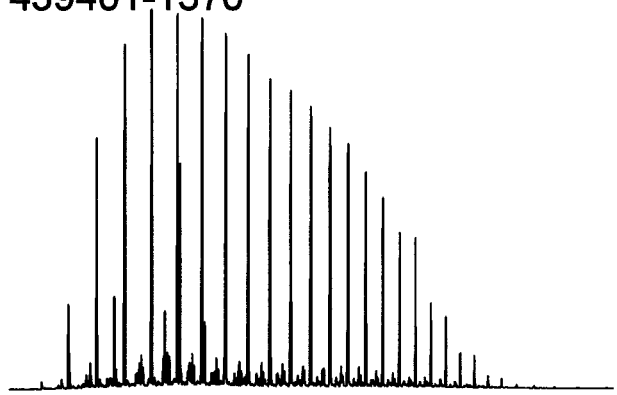

439401-1180

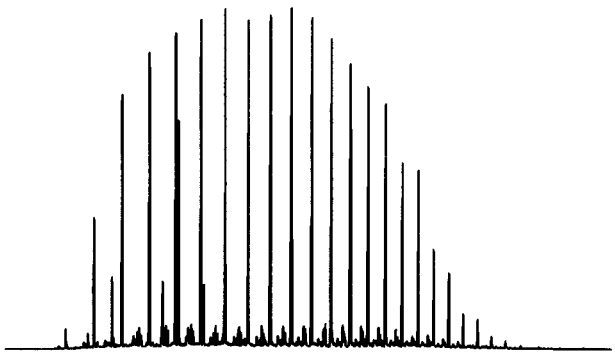

439401-1440

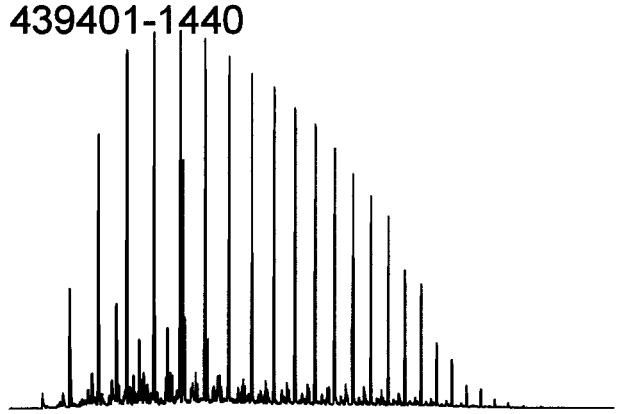

439401-1230

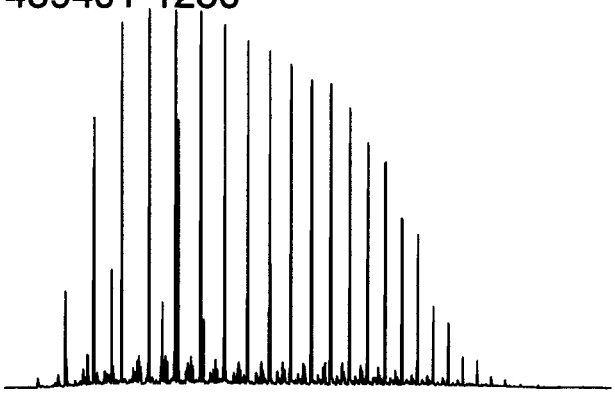

439401-1485

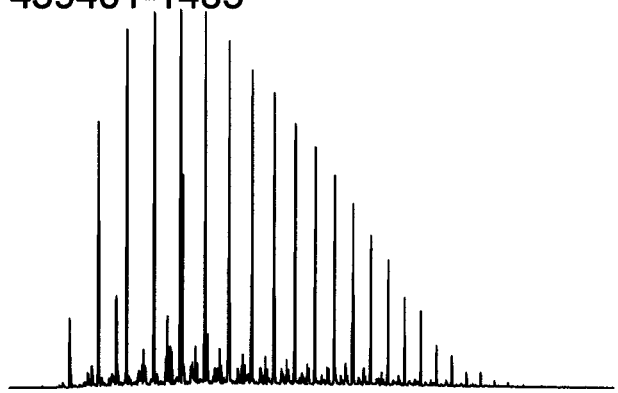

439401-1250

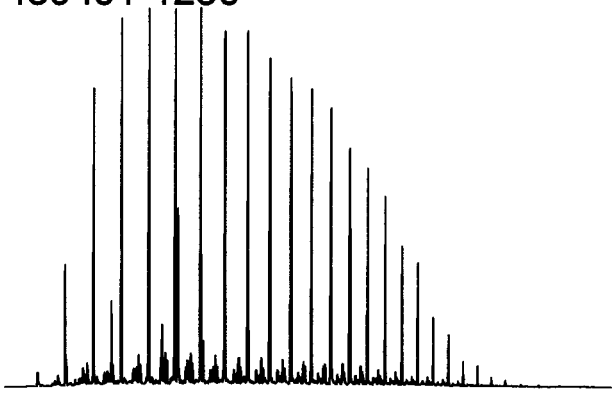

439401-1545

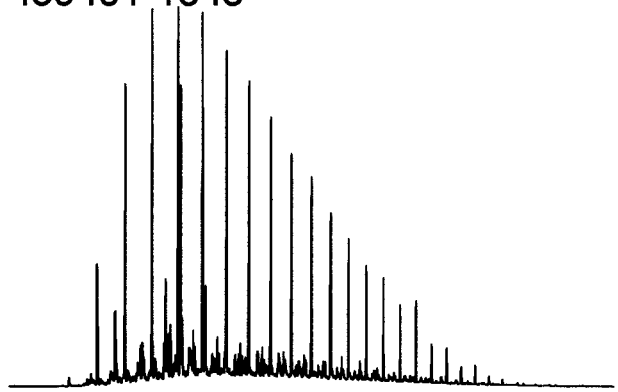

Fig. 9 continued

439401-1725

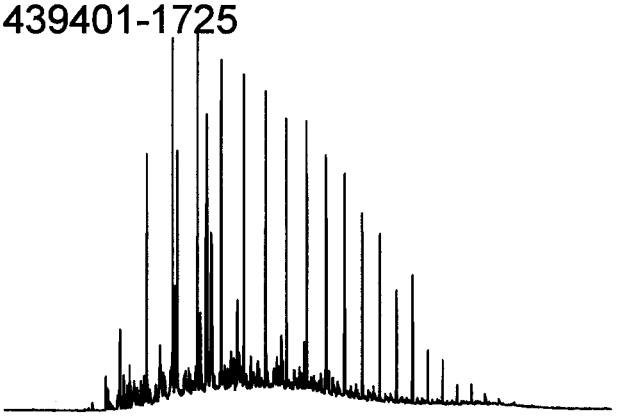

439401-2510

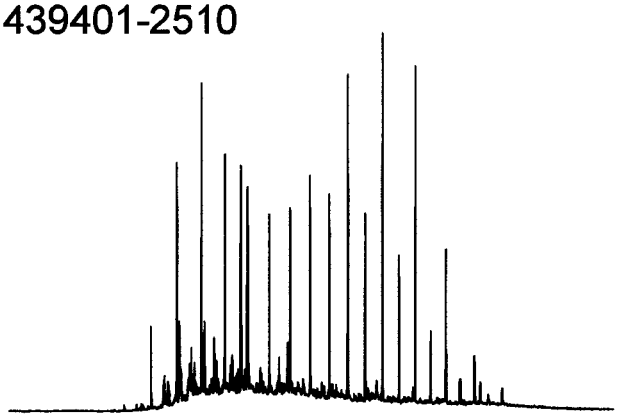

439401-1830

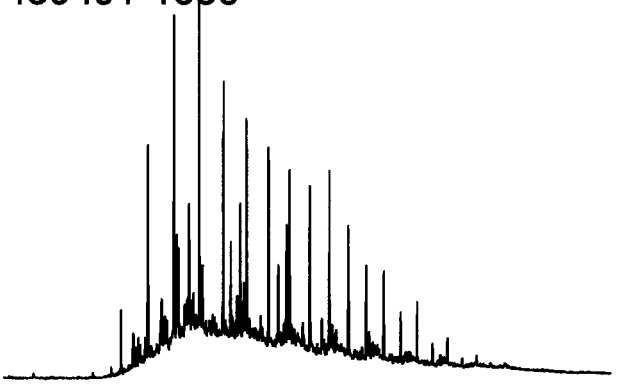

439401-2875

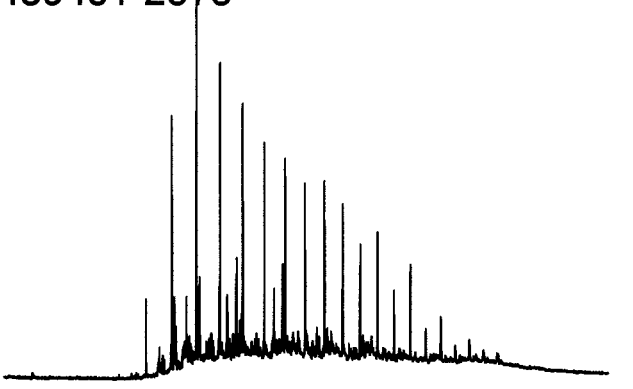

439401-2145

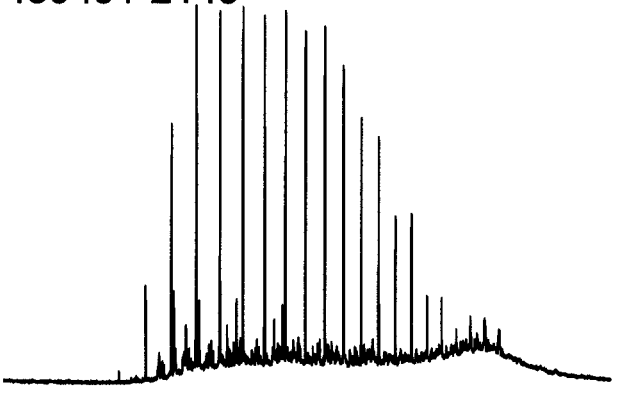

439401-2950

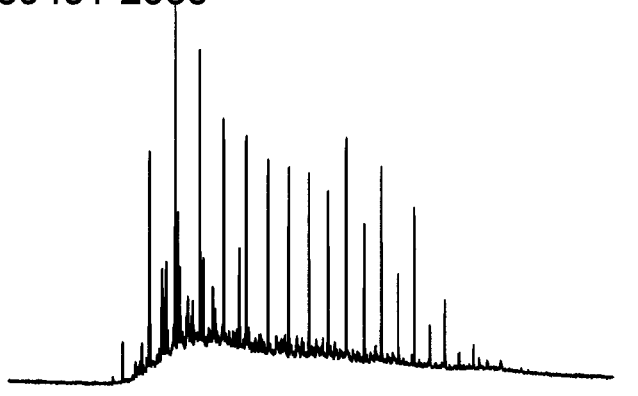

439401-2300

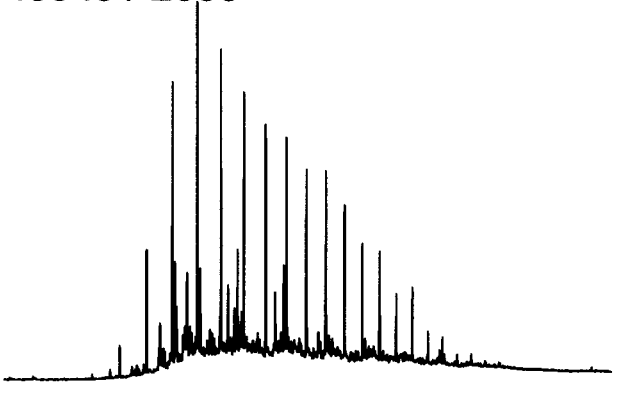

Fig. 9 continued

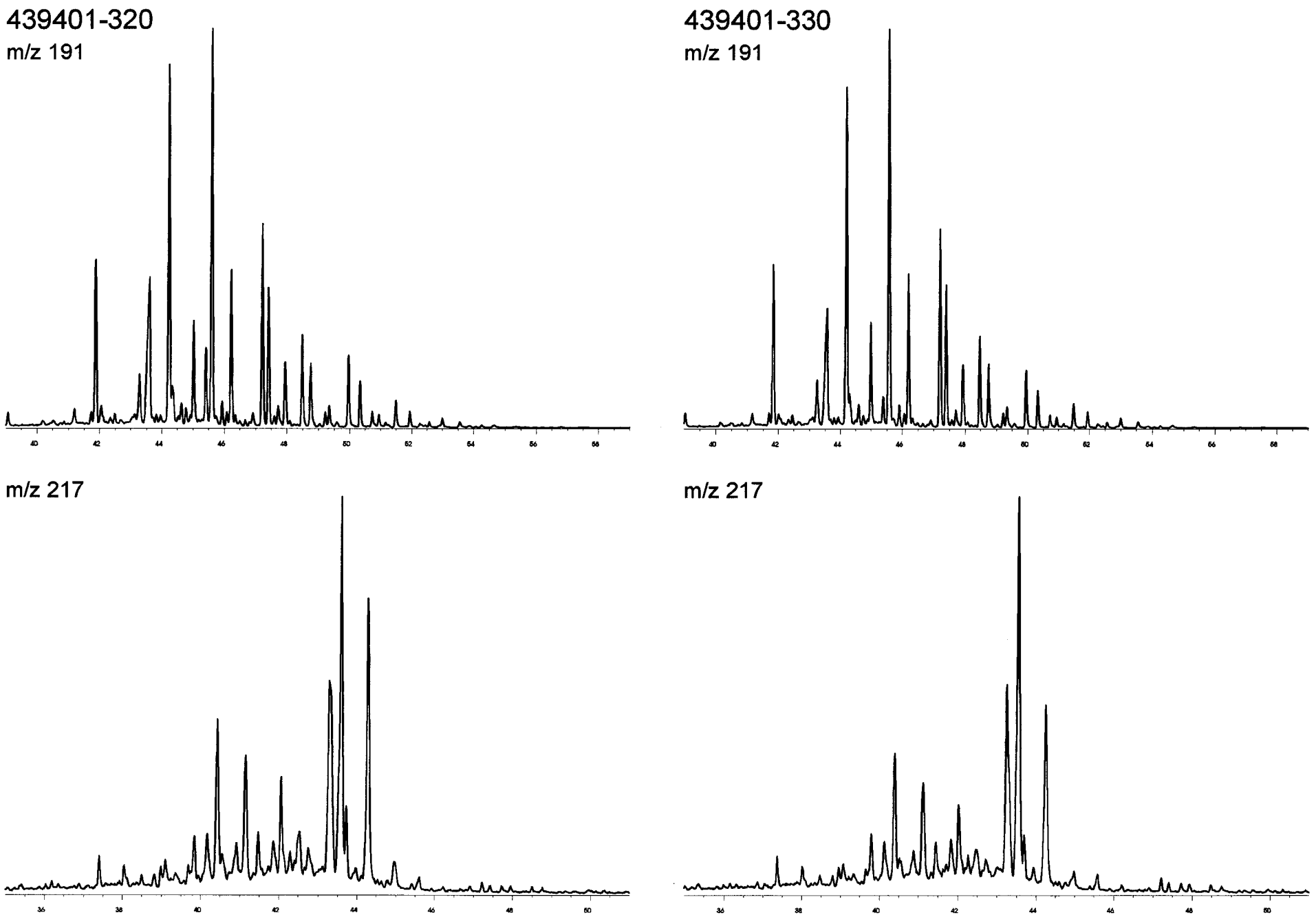

Fig. 10

439401-340

m/z 191

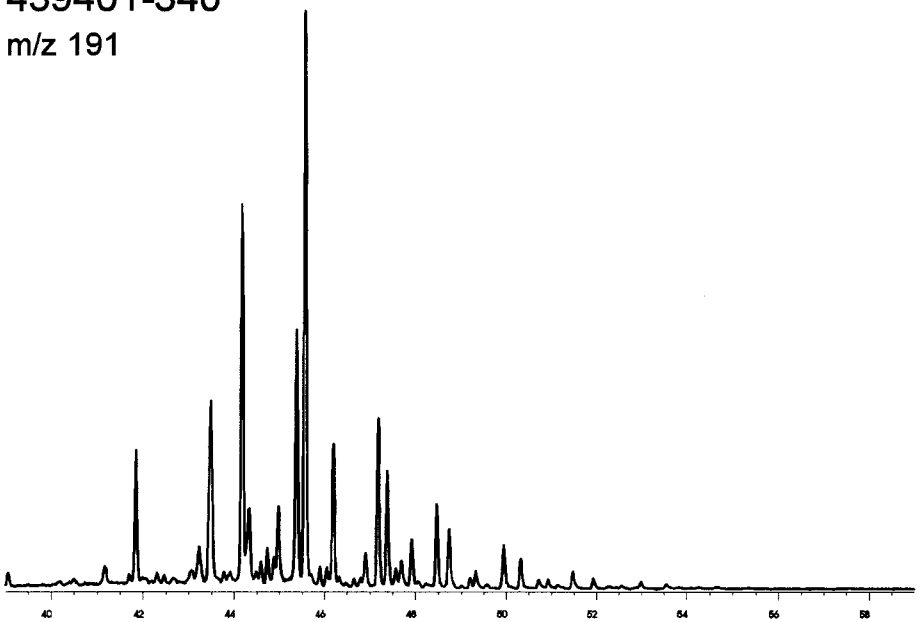

439401-350

m/z 191

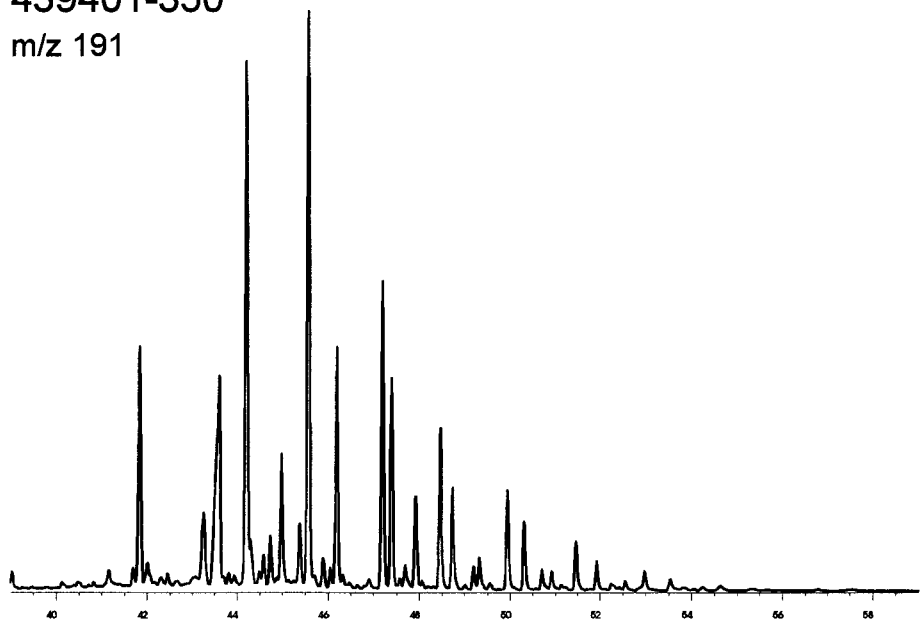

m/z 217

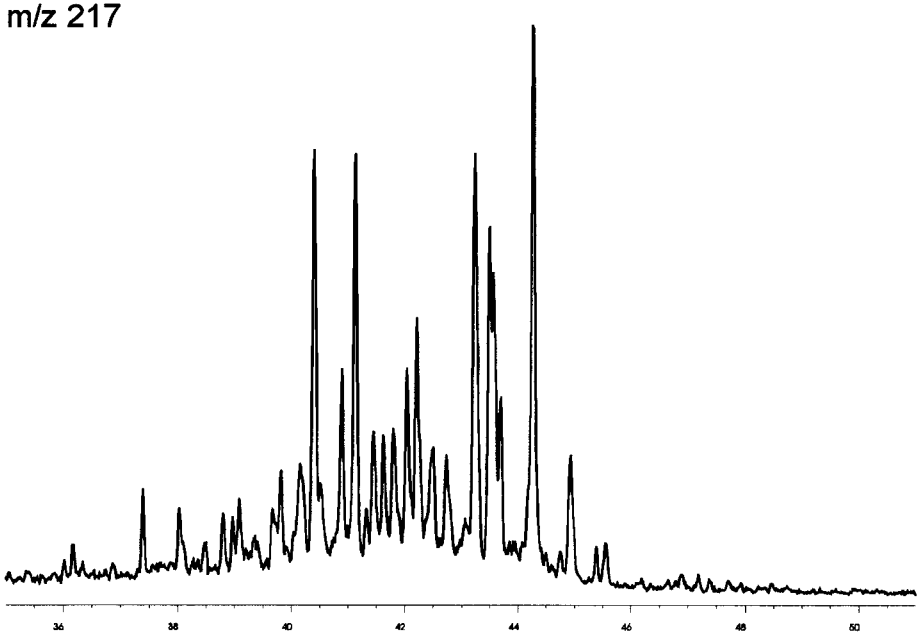

m/z 217

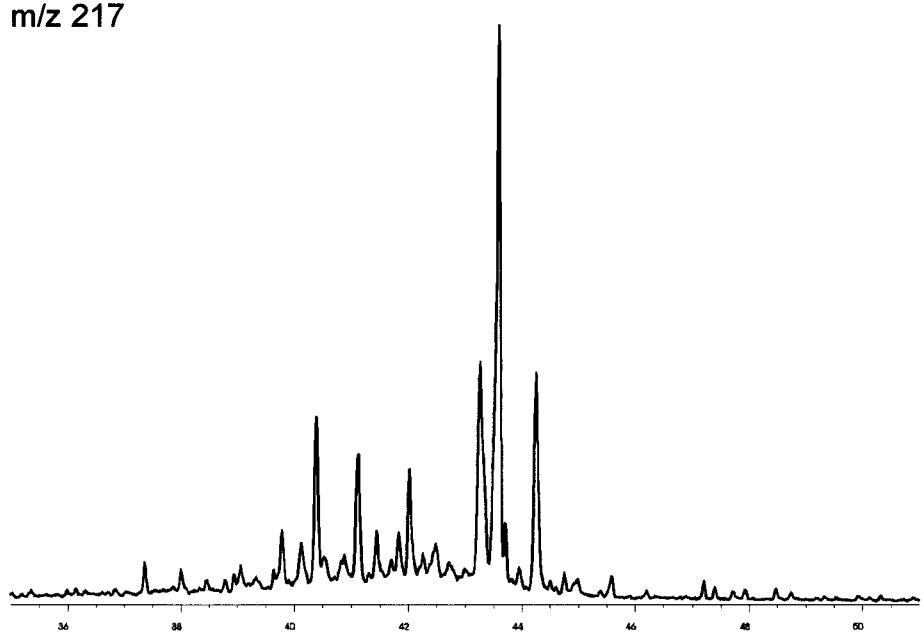

Fig. 10 continued

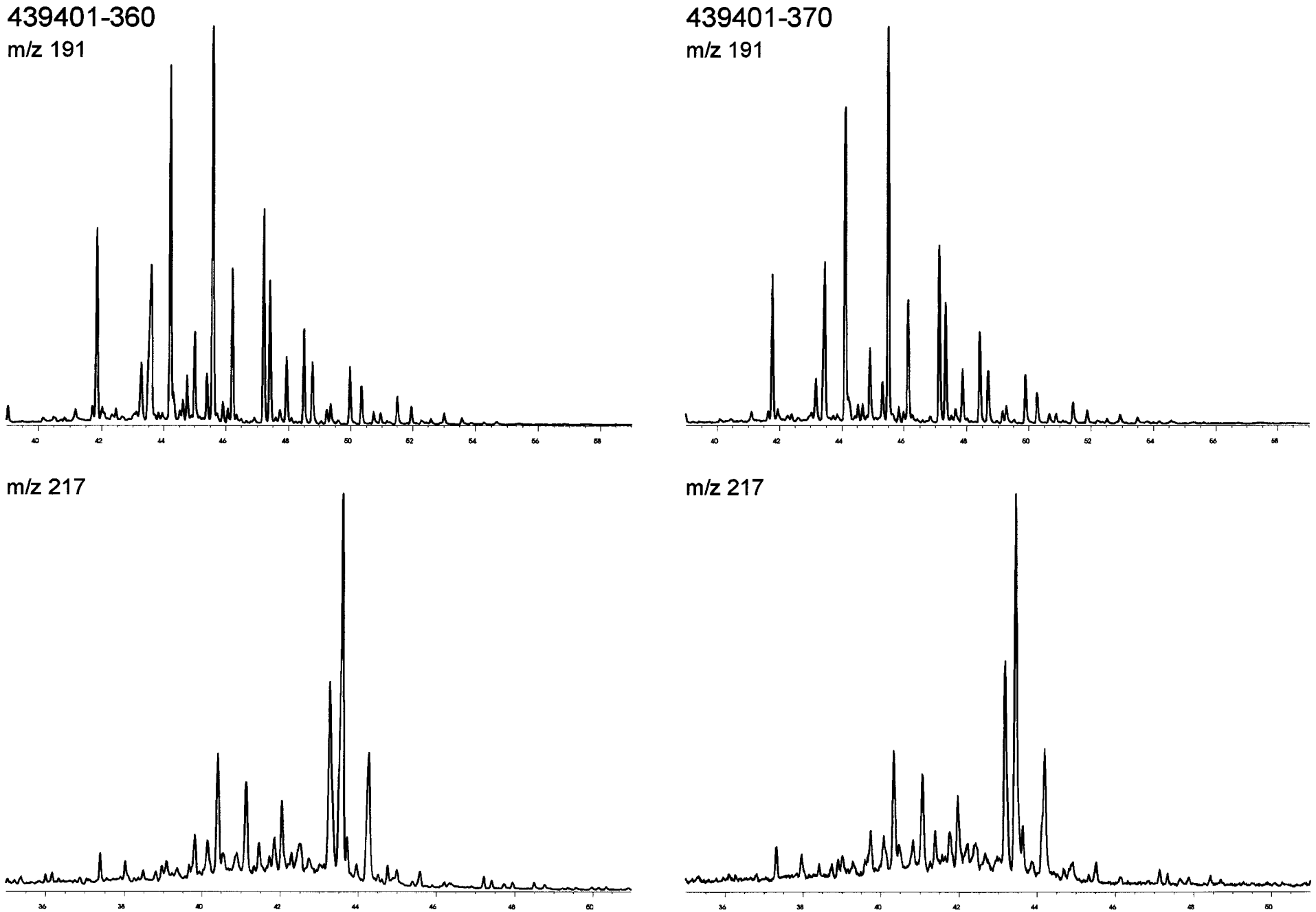

Fig. 10 continued

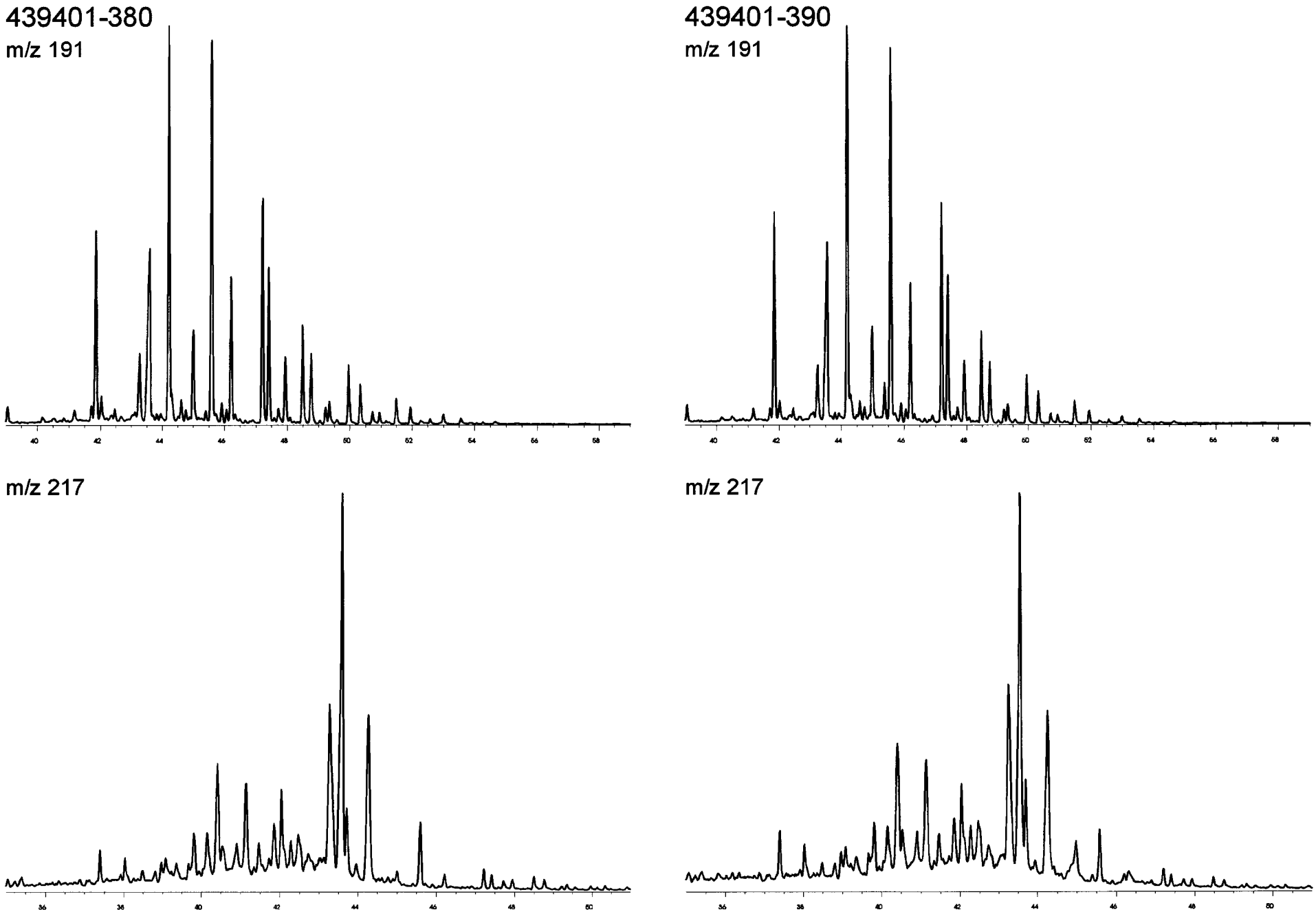

Fig. 10 continued

439401-400

m/z 191

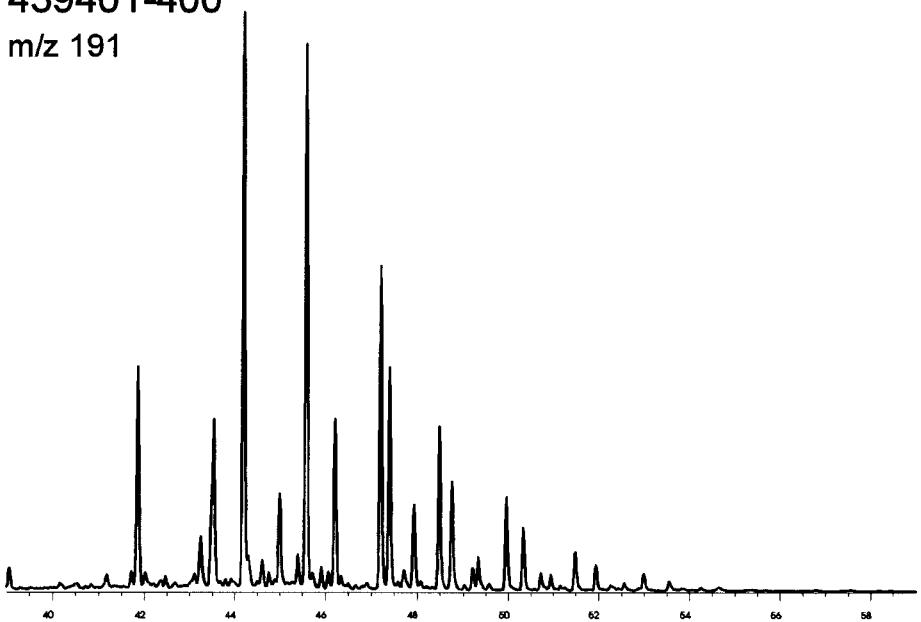

439401-410

m/z 191

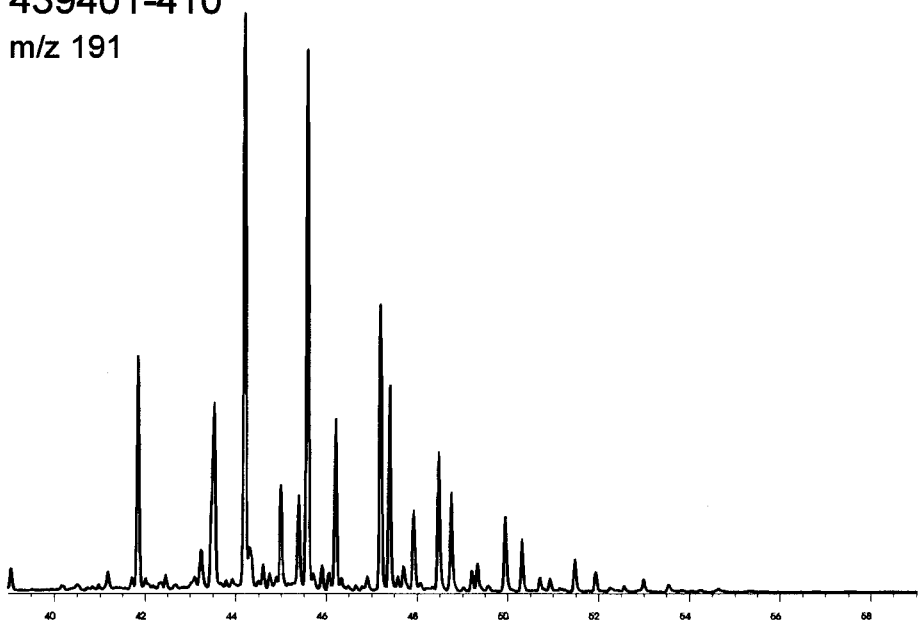

m/z 217

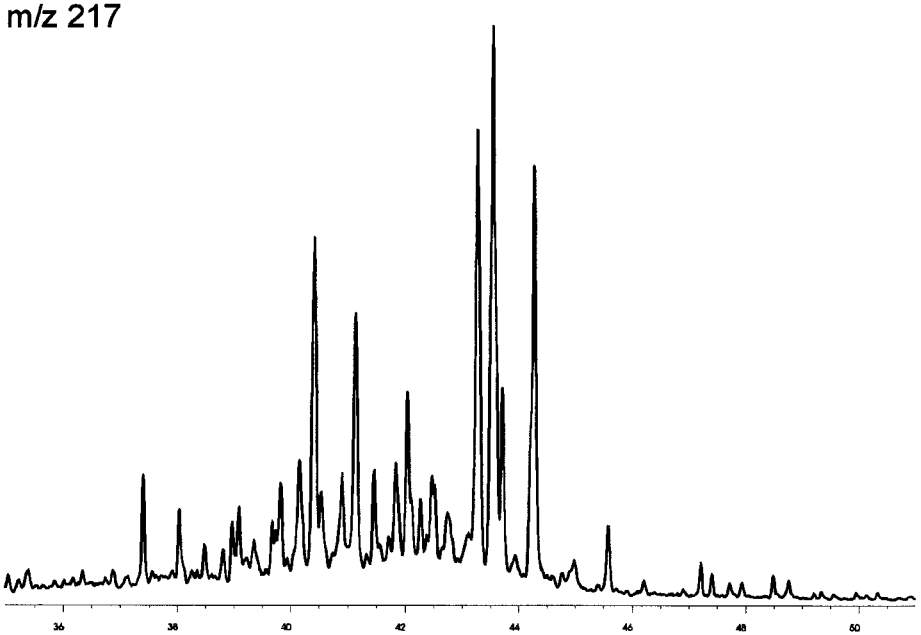

m/z 217

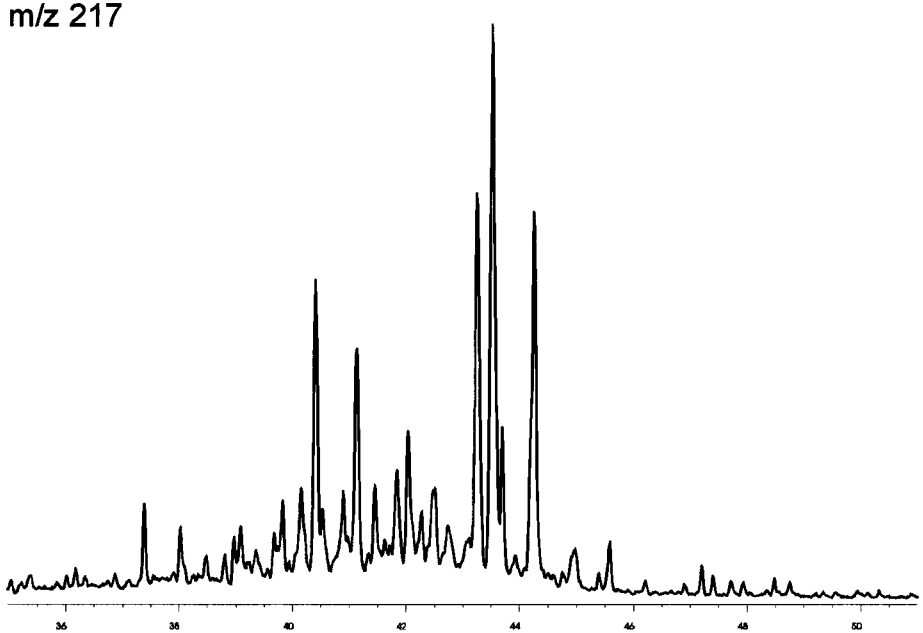

Fig. 10 continued

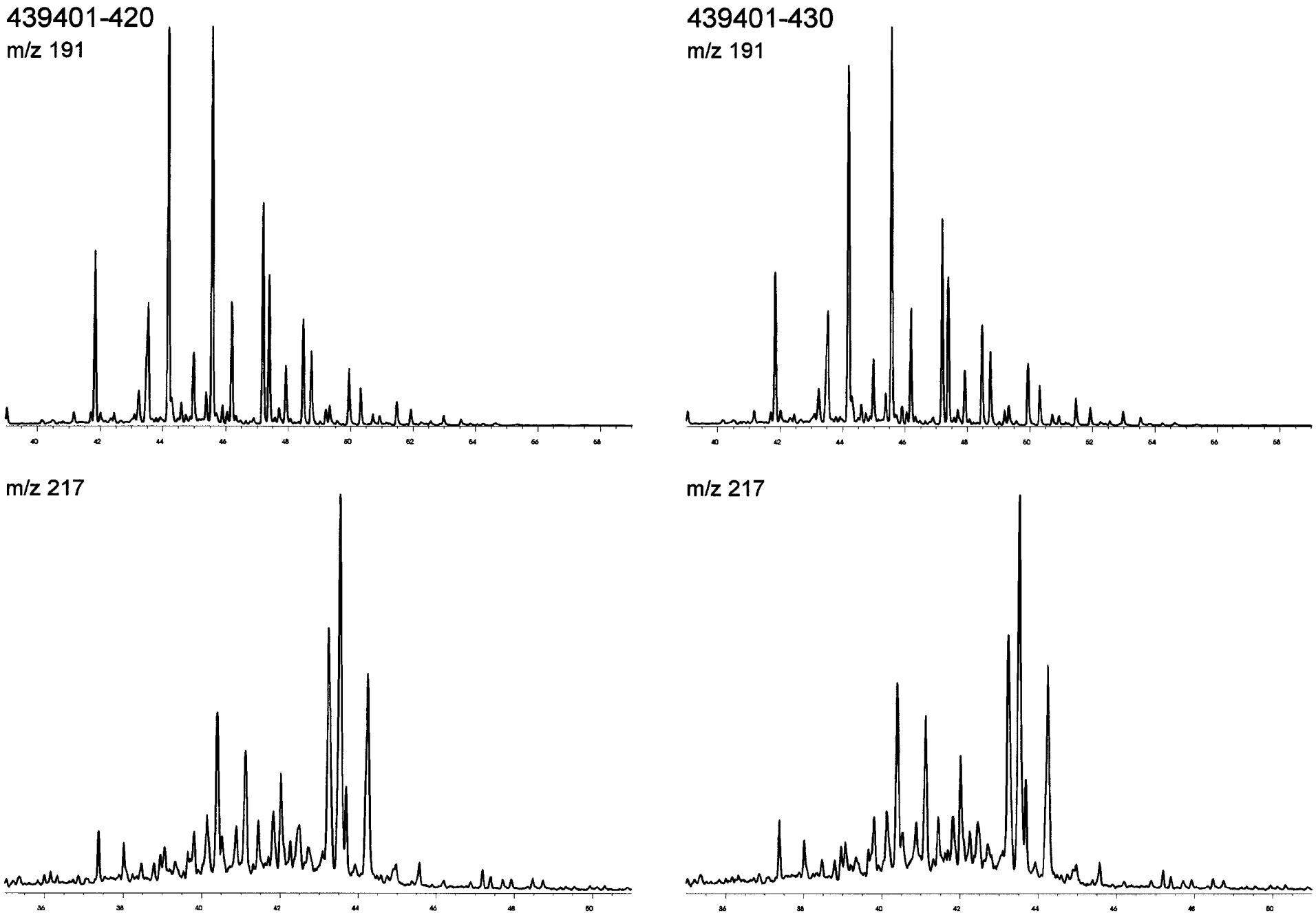

Fig. 10 continued

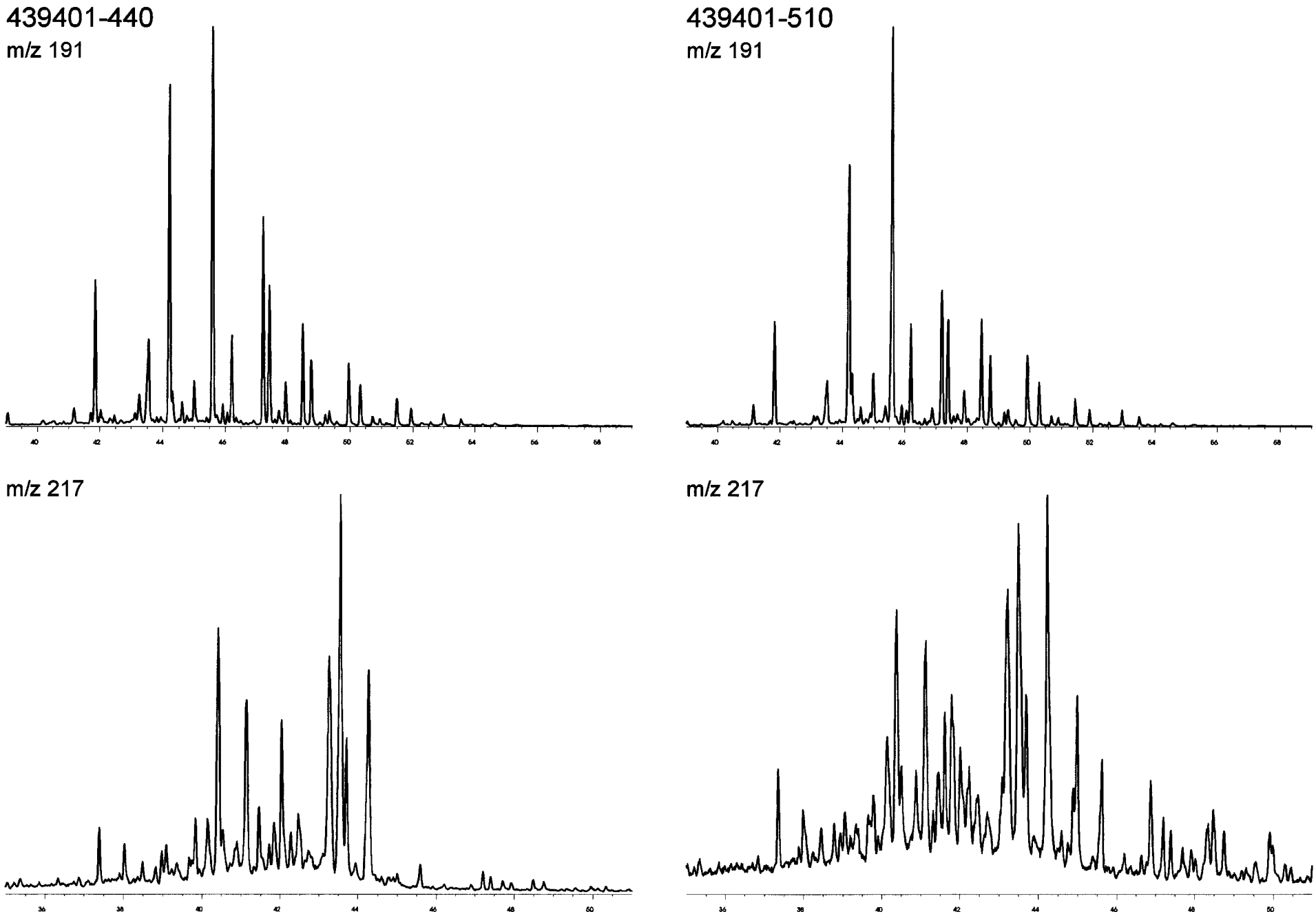

Fig. 10 continued

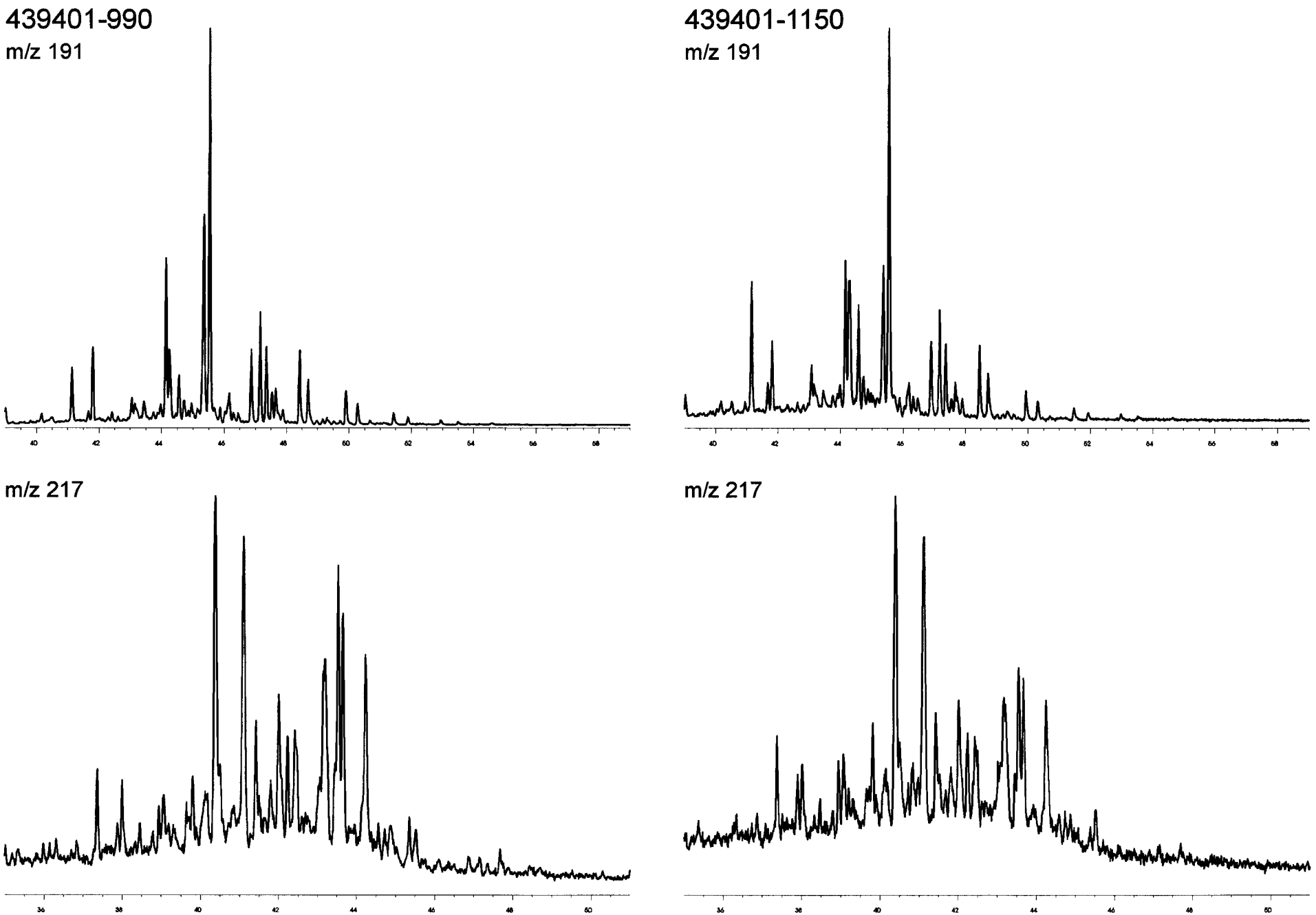

Fig. 10 continued

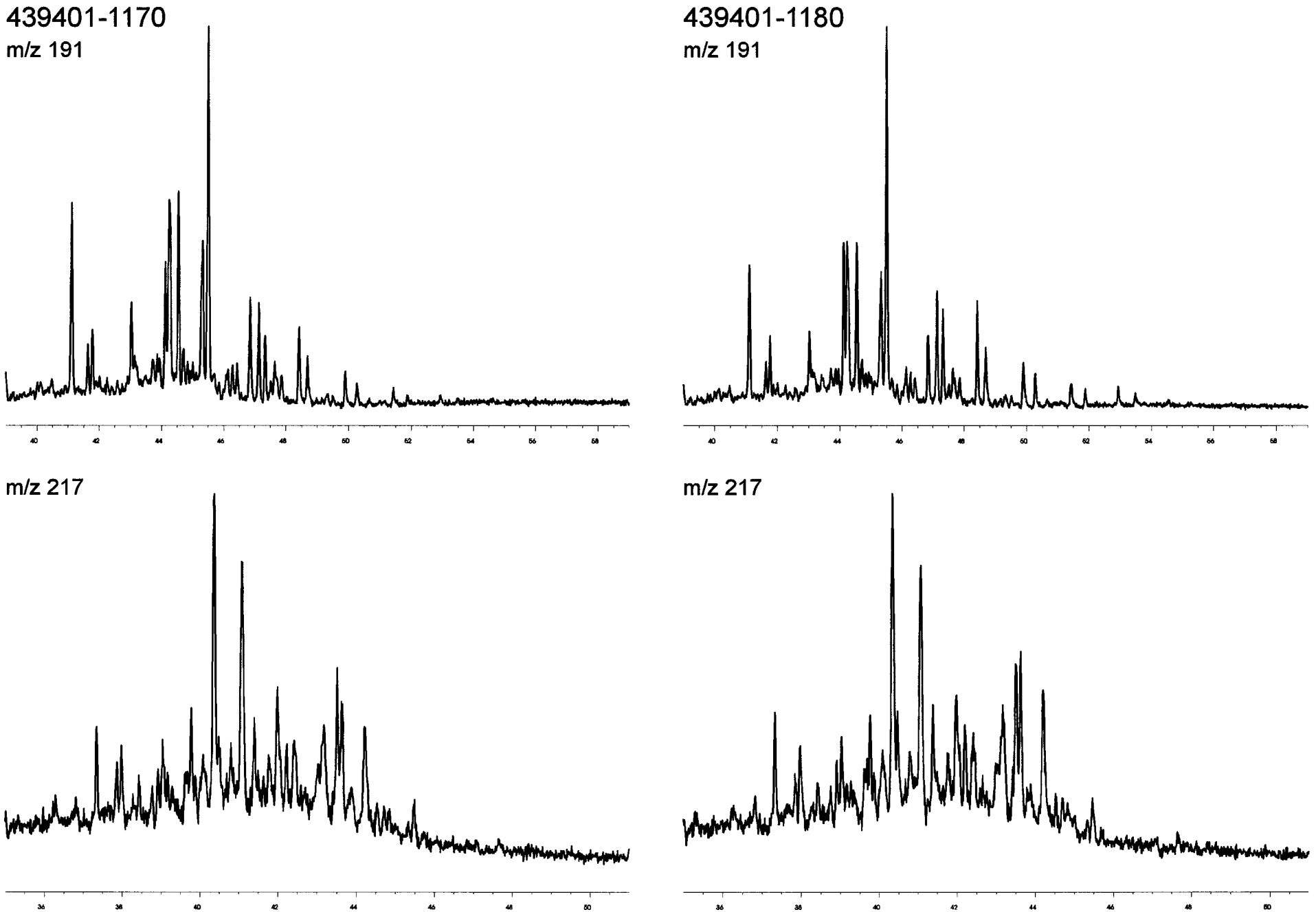

Fig. 10 continued

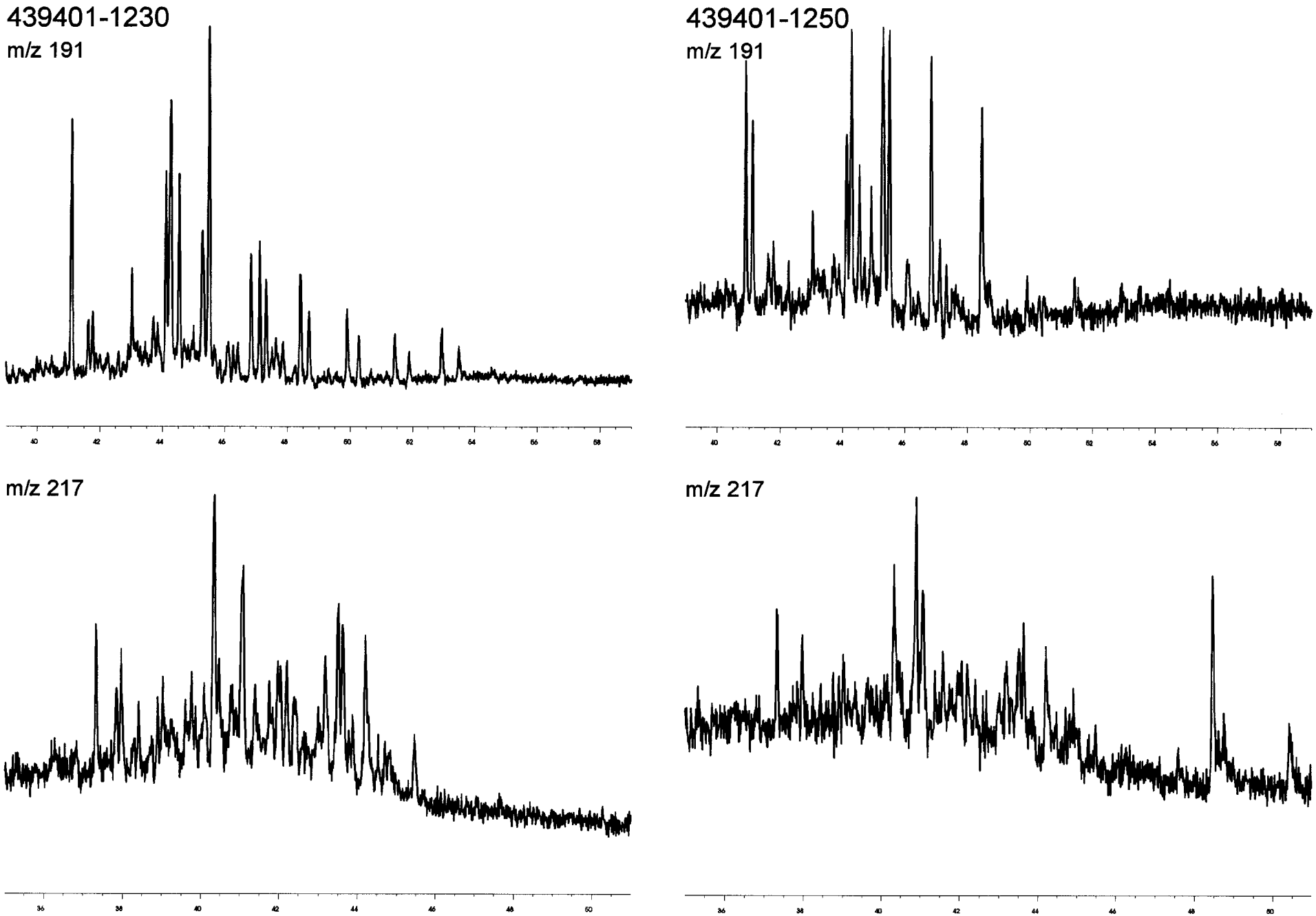

Fig. 10 continued

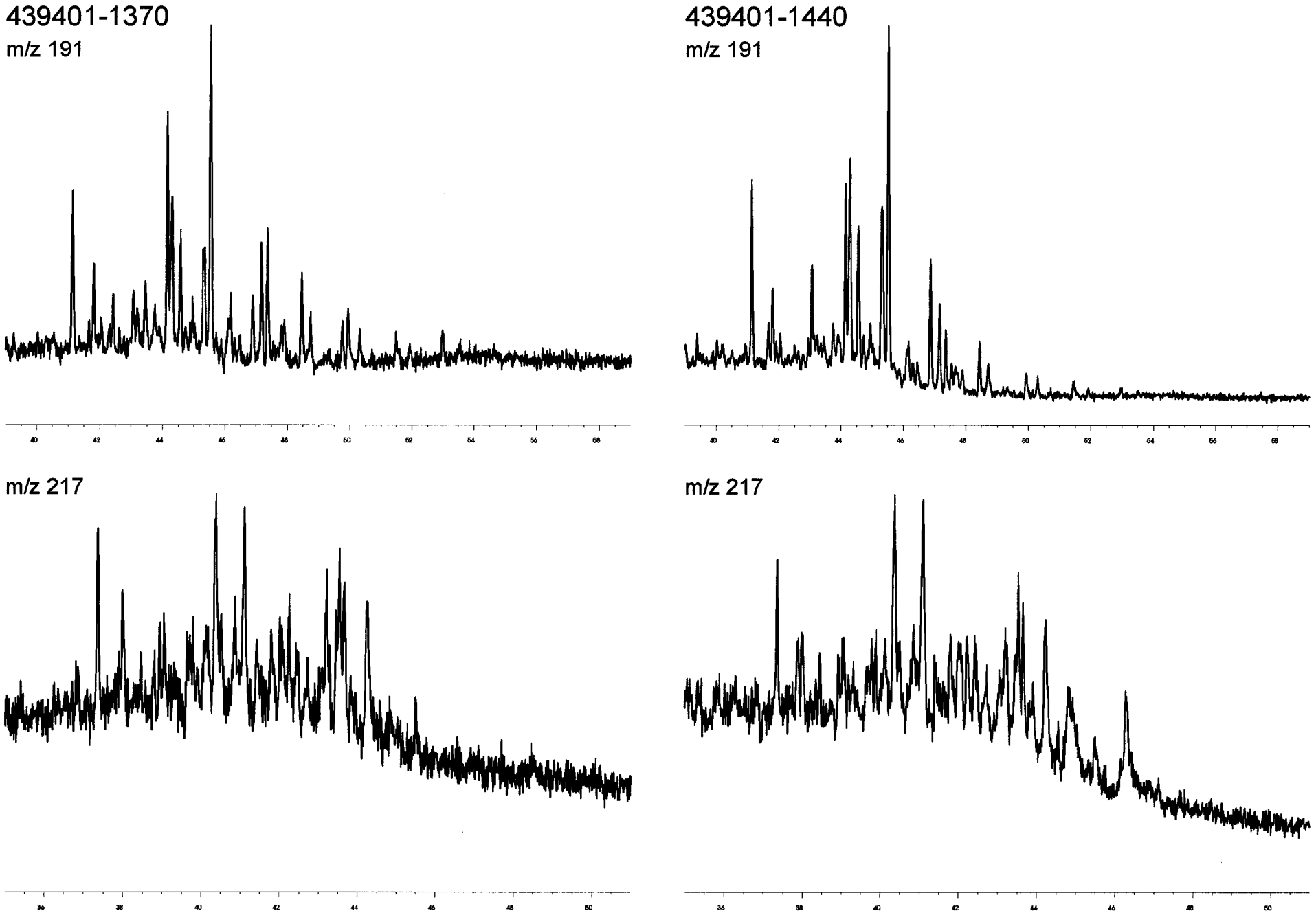

Fig. 10 continued

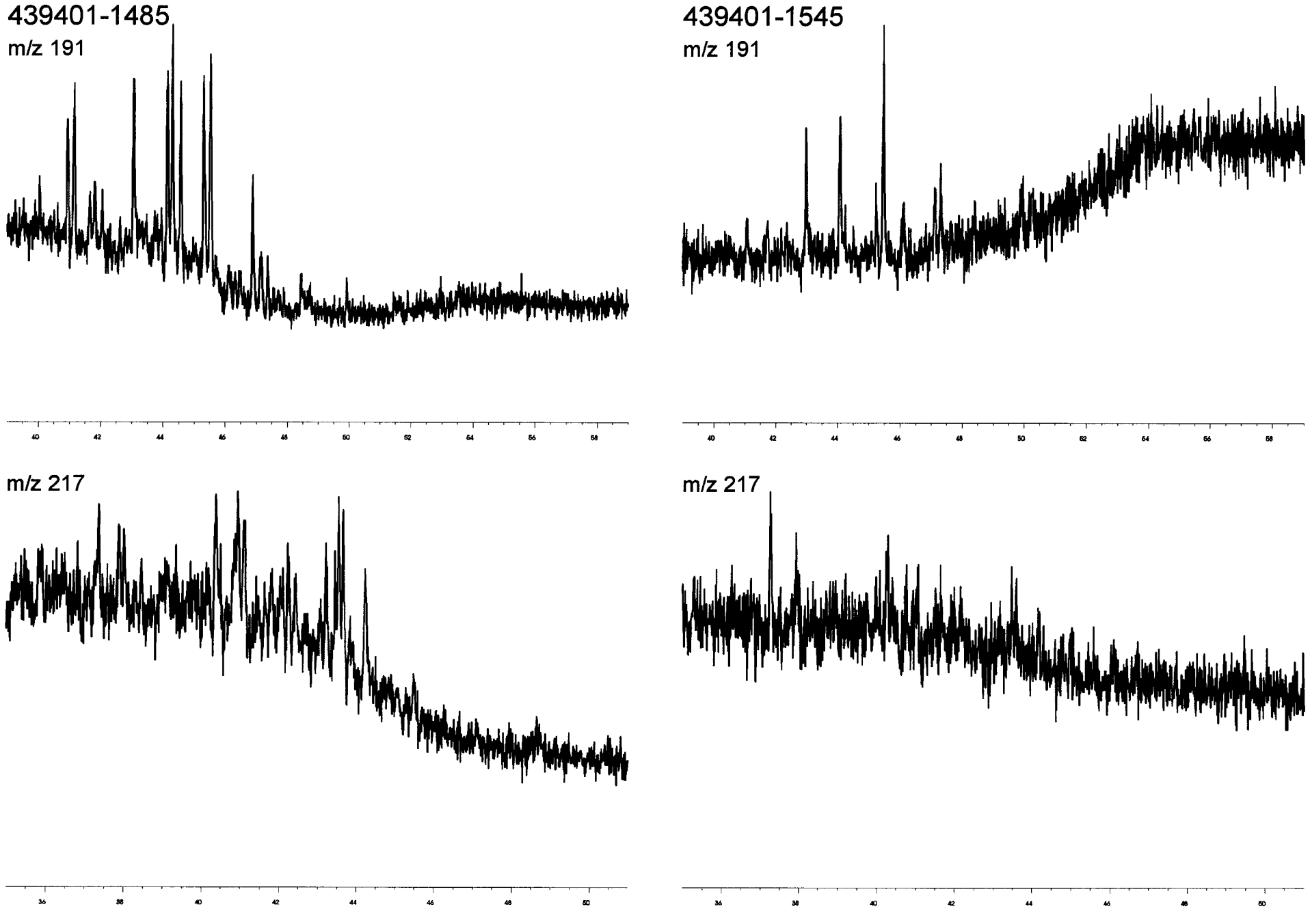

Fig. 10 continued

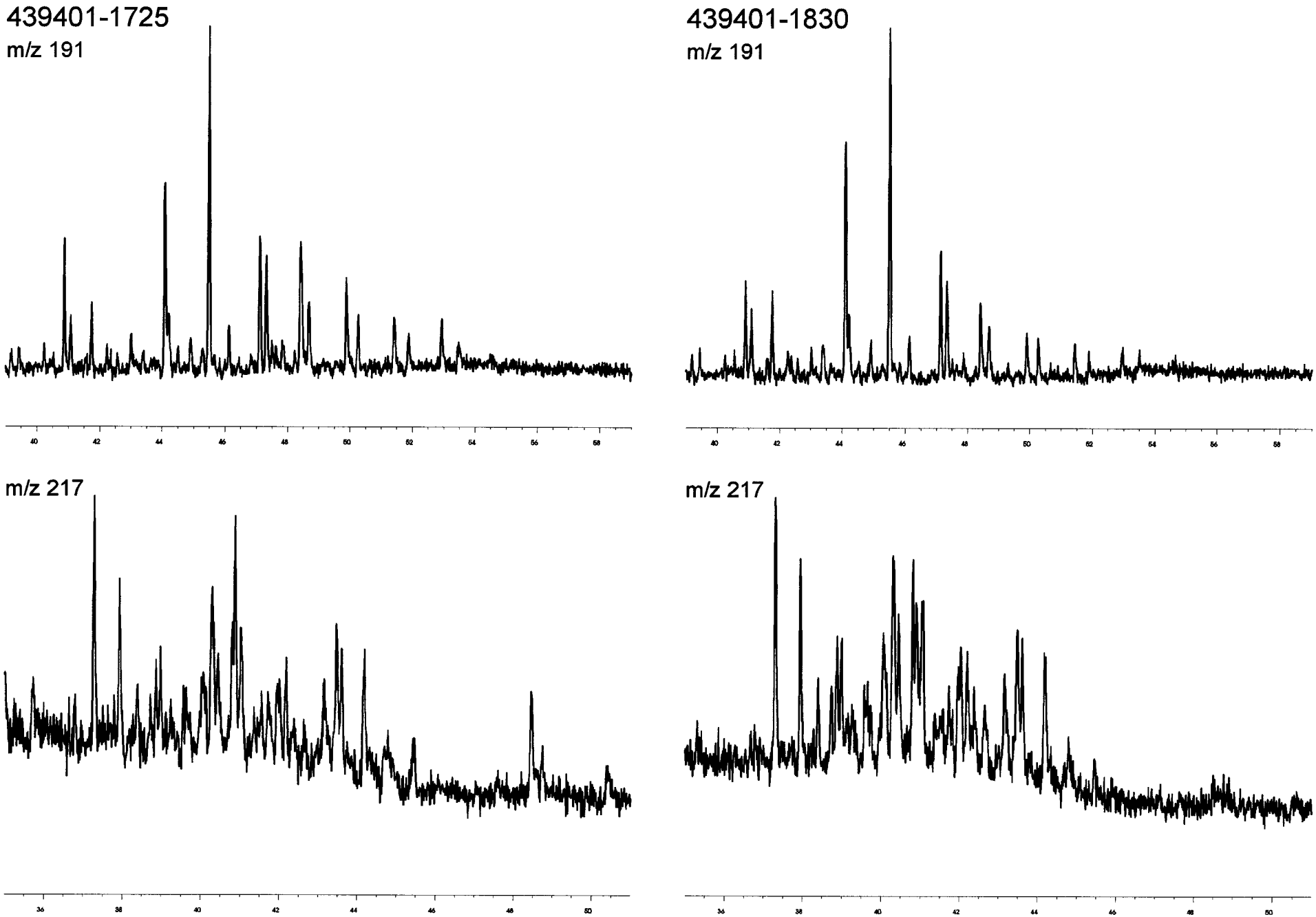

Fig. 10 continued

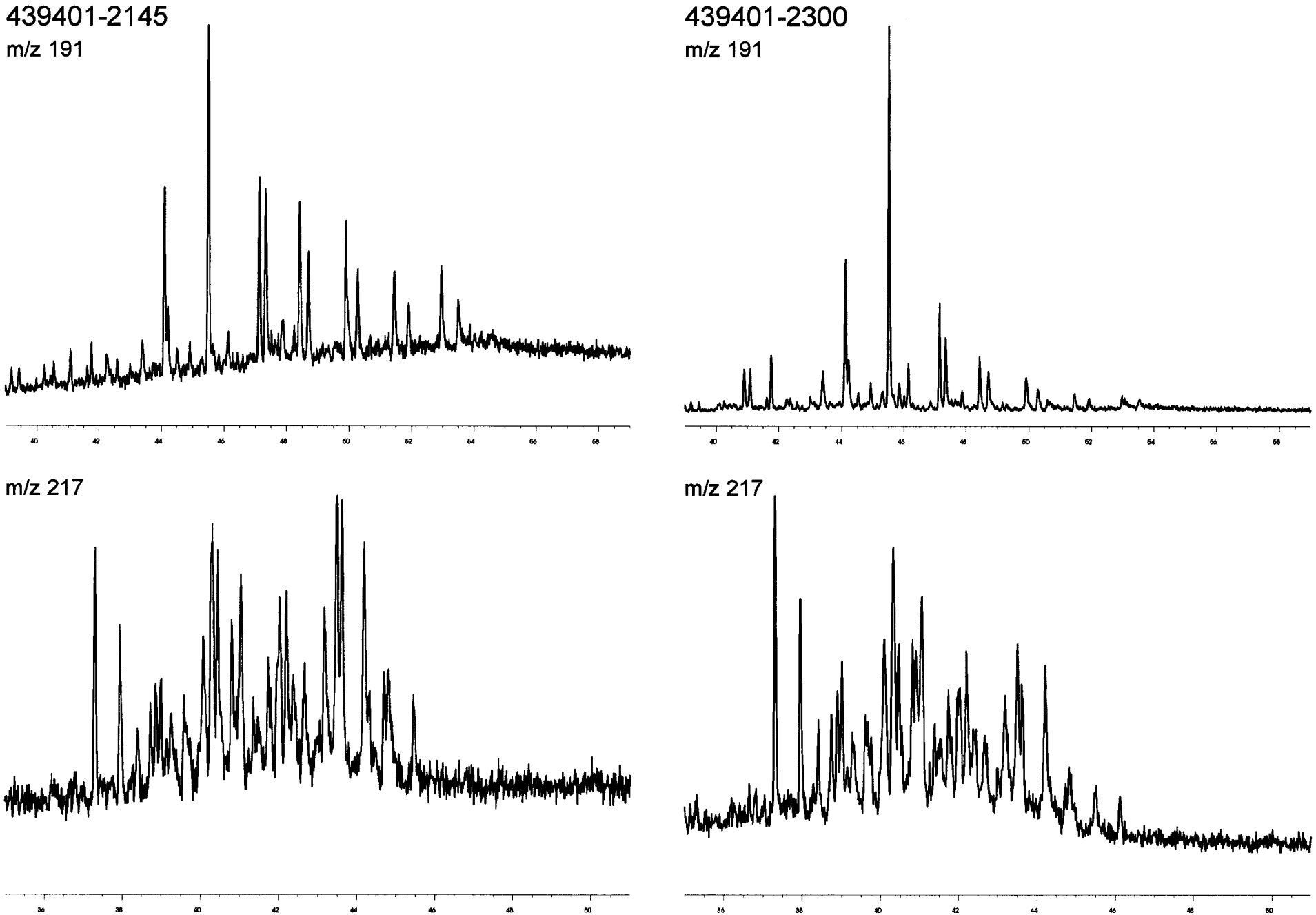

Fig. 10 continued

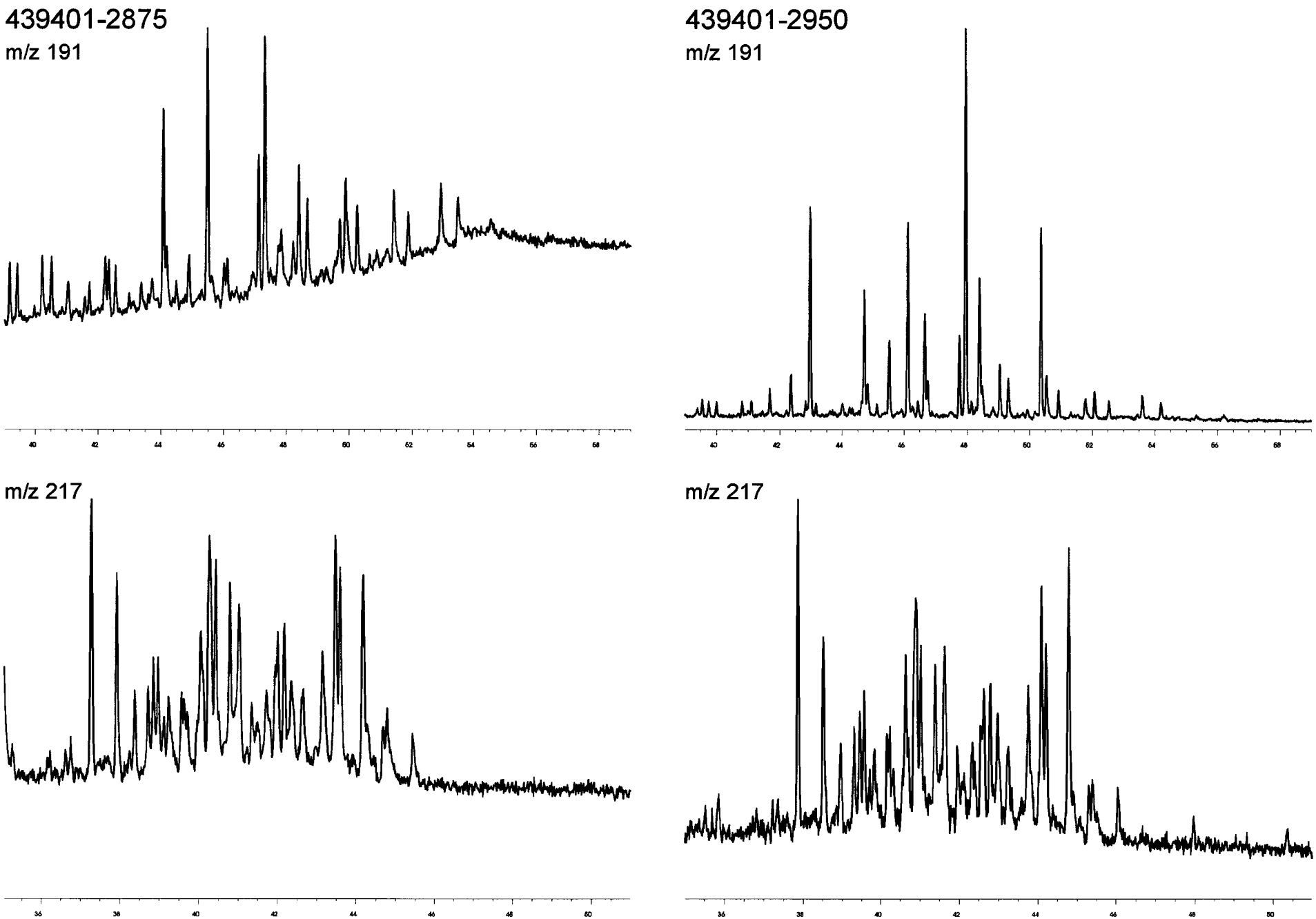

Fig. 10 continued

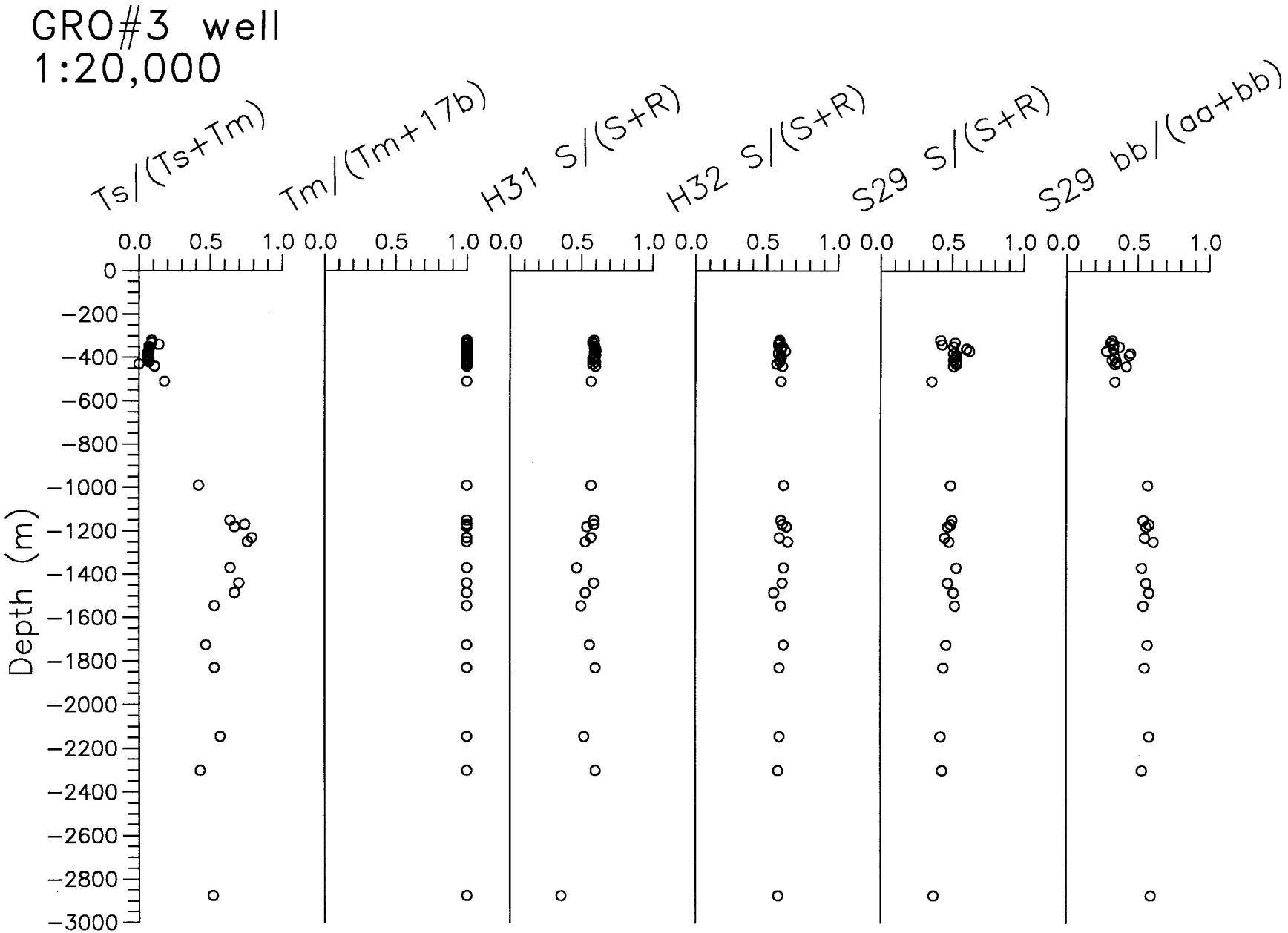
GRO#3 well
1:20,000
Ts/(Ts+Tm)
Tm/(Tm+17b)
H31 S/(S+R)
H32 S/(S+R)
S29 S/(S+R)
S29 bb/(aa+bb)
0.0
0.5
1.0
Depth (m)
0
−200
−400
−600
−800
−1000
−1200
−1400
−1600
−1800
−2000
−2200
−2400
−2600
−2800
−3000

Fig. 11

Table 1.

Well data for grønArctic Nuussuaq Kugssuaq GRO #3

Well name:	Nuussuaq Kugssuaq GRO #3
Classification:	Exploration
Operator:	grønArctic Energy Inc., Calgary, Alberta, Canada
Drilling contractor:	Terroco Drilling Ltd.
Drilling rig:	Terroco Rig 1
Logging contractor:	Schlumberger
Mud logging contractor:	Sperry-Sun Drilling Services of Canada
Drill stem test contractor:	Alpine Testers
Locality:	Western tip of Nuussuaq peninsula, western Greenland
Co-ordinates:	70°27.765' N 54°05.227' W
Ground elevation:	17.6 m a. s. l.
Kelly bushing:	22.5 m a. s. l.
Well spud:	3 August 1996
Termination:	17 September 1996
Rig released:	5 October 1996
Total depth:	Driller 2996.7 m
Total depth:	Schlumberger 2995.5
Hole diameter:	660 mm 0 - 33 m 455 mm 33 - 247 m 311 mm 247 - 801 m 216 mm 801 - 2996.7 m
Core:	No core taken
Sidewall core:	No sidewall cores taken
Logs:	A full suite of petrophysical wireline logs and a VSP (vertical seismic profile) were acquired
Formation drilled:	The drilling and wireline logs recorded 312 m of basalt at top and sand and shale successions from 312 m to TD
Hydrocarbons:	A number of sand intervals contained hydrocarbons
Test:	Eight of the most prospective zones were drill stem tested
Status:	Plugged and abandoned

Screening data

Depth	TOC(%)	S1	S2	HI	Tmax	Ro
320	2,97	0,47	5,38	181	432	0,71
330	3,62	0,66	6,54	181	431	
340	2,06	0,76	3,26	158	437	
350	3,71	0,70	8,06	217	433	
360	3,96	0,61	8,08	204	432	0,72
370	2,54	0,49	2,46	97	439	0,77
380	3,12	0,32	4,30	138	437	
390	2,45	0,20	2,68	109	437	
400	3,68	0,34	4,46	121	437	0,74
410	3,26	0,32	3,82	117	438	
420	3,80	0,38	4,80	126	437	
430	2,82	0,31	3,70	131	437	
440	3,23	0,48	4,50	139	436	
450	1,75	0,26	2,20	126	438	
510	1,21	0,18	1,03	85	442	
990	4,03	0,74	5,00	124	442	
1110						0,98
1150	5,89	1,14	6,86	116	450	1,02
1150	5,50	1,08	6,82	124	452	0,97
1160	4,45	0,87	3,96	89	454	
1170	5,73	1,03	6,04	105	451	
1180	3,97	0,68	3,82	96	452	
1190	3,13	0,42	1,64	52	456	
1200	3,64	0,51	2,56	70	457	1,15
1210	4,82	0,74	3,72	77	457	
1210	4,36	0,70	3,40	78	459	
1220	5,01	0,92	3,62	72	457	
1230	4,69	0,82	3,92	84	456	1,02
1230	4,50	0,75	3,66	81	459	
1240	4,68	0,89	3,82	82	461	
1250	4,50	0,74	3,06	68	461	1,32
1250	4,38	0,96	2,47	56	473	
1260	3,98	0,49	1,84	46	465	
1260	3,00	0,39	0,90	30	469	
1290	5,61	0,71	2,02	36	469	
1300						1,23
1310	5,36	0,72	4,04	75	458	
1320	4,68	0,63	3,60	77	459	
1350	3,96	0,69	2,94	74	459	
1360	2,41	0,24	0,88	37	469	
1370	5,62	0,82	4,12	73	463	
1380	5,30	0,76	3,74	71	465	
1390						1,23

Table 2

1400	5,42	0,81	3,88	72	462	
1410	5,38	0,71	3,48	65	465	
1420	4,93	0,58	3,26	66	465	
1430	5,47	0,62	3,22	59	468	
1440	5,02	0,66	3,04	61	461	1,28
1450	4,78	0,49	2,86	60	469	
1460	5,53	0,51	3,16	57	470	
1470	5,35	0,55	3,38	63	470	
1485	6,55	0,75	4,10	63	475	1,36
1525	5,24	0,51	2,80	53	472	
1535	4,70	0,47	2,44	52	477	
1545	3,91	0,48	1,94	50	477	1,42
1560	4,14	0,25	1,84	44	481	
1570	3,86	0,30	1,76	46	487	
1585	3,81	0,24	1,74	46	490	1,46
1650	1,98	0,16	0,98	49	485	
1650	4,26	0,30	2,08	49	485	
1725	3,91	0,53	1,40	36	501	1,62
1730	4,43	0,25	1,52	34	484	
1770	5,09	0,16	1,44	28	499	
1780	5,41	0,16	1,60	30	493	
1790	6,15	0,16	1,48	24	498	
1800	5,66	0,15	1,42	25	521	
1810	6,01	0,16	1,50	25	530	
1820	6,08	0,17	1,54	25	528	
1830	6,38	0,16	1,64	26	524	1,87
1840	5,58	0,21	1,42	25	530	
1855	6,21	0,16	1,70	27	523	
1890	4,97	0,09	1,12	23	528	
1935	6,44	0,16	1,18	18	528	1,95
1950	4,95	0,14	0,92	19	528	
1970	6,15	0,12	1,10	18	536	
1985	5,10	0,11	1,14	22	535	
2000	5,57	0,11	1,08	19	539	
2030	4,34	0,10	0,84	19	534	
2050	4,37	0,07	0,88	20	537	
2145	5,03	0,07	0,96	19	544	1,90
2185	4,71	0,07	0,48	10	555	
2190	4,01	0,05	0,34	8	560	
2200	5,88	0,06	0,84	14	552	
2215	4,20	0,04	0,44	10	550	
2240	5,32	0,04	0,64	12	555	2,13
2255	4,33	0,08	0,46	11	558	
2270	4,63	0,03	0,38	8	560	
2285	4,16	0,04	0,38	9	560	
2300	4,78	0,05	0,38	8	559	2,15
2335	4,53	0,04	0,36	8	557	
2350	5,02	0,06	0,54	11	554	
2360	5,78	0,03	0,42	7	565	

Table 2 continued

2365						2,24
2375	4,16	0,04	0,38	9	557	
2395	4,98	0,03	0,52	10	559	2,15
2435						2,29
2450	2,84	0,03	0,26	9	563	
2470	4,84	0,05	0,24	5	568	
2490	5,15	0,04	0,42	8	564	
2510	4,21	0,08	0,32	8	564	2,25
2530	3,94	0,01	0,30	8	566	
2550	4,67	0,04	0,28	6	568	
2565	4,69	0,05	0,20	4	570	
2580	4,37	0,01	0,20	5	572	
2590	4,20	0,04	0,20	5	573	
2605	4,52	0,01	0,18	4	573	2,53
2630	1,15	0,02	0,06	5		
2700	5,60	0,02	0,28	5	570	
2710	5,14	0,02	0,08	4	574	2,63
2710						2,55
2720	4,79	0,03	0,20	4	572	
2730	4,68	0,02	0,24	5	572	
2740	4,80	0,03	0,26	5	573	
2750	4,64	0,01	0,04	6	571	
2760	4,70	0,03	0,28	6	571	
2820	2,37	0,01	0,14	6	571	
2875	4,33	0,06	0,20	5	575	2,57
2910	4,53	0,03	0,18	4	575	
2930	3,69	0,04	0,16	4	571	
2950	4,55	0,20	0,18	4	573	2,63
2990	2,74	0,04	0,22	8	560	

Table 2 continued

Solvent extraction data

Sample	Lab. No.	Ext. yield (mg/g OC)	Asphaltenes (%)	Sat (%)	Aro (%)	Polars (%)	Sat/Aro
439401-320	97001-20	56	42	25,8	31,6	42,6	0,82
439401-330	97001-21	50	42,1	18,4	21,7	59,9	0,85
439401-340	97001-93	89	25,4	50,5	15,1	34,4	3,34
439401-350	97001-94	46	42,9	21,8	17,7	60,5	1,23
439401-360	97001-22	47	46	18,2	18,2	63,5	1,00
439401-370	97001-15	65	33,8	19,1	13,2	67,6	1,45
439401-380	97001-23	42	47,3	15,8	9,9	74,3	1,60
439401-390	97001-24	37	42,2	22,8	12,7	64,6	1,80
439401-400	97001-25	28	43,5	18,2	7,8	74	2,33
439401-410	97001-26	25	42,4	19,4	9,7	70,8	2,00
439401-420	97001-27	28	40	20,9	8,8	70,3	2,38
439401-430	97001-28	32	38,6	23,2	11	65,9	2,11
439401-440	97001-29	50	31,7	20,6	12,1	67,3	1,70
439401-510	97001-16	43	22,8	23,3	11,6	65,1	2,01
439401-990	97001-31	25	37,6	26	7,3	66,7	3,56
439401-1150	97001-32	35	37,7	35,3	7,8	56,9	4,53
439401-1170	97001-33	30	31,5	33,3	9,2	57,5	3,62
439401-1180	97001-34	29	31,6	27	6,7	66,3	4,03
439401-1230	97001-37	32	31,2	35,7	7	57,3	5,10
439401-1250	97001-17	27	18,6	32,6	12	55,4	2,72
439401-1370	97001-102	9	32	35,2	5,6	59,3	6,29
439401-1440	97001-45	21	31,9	31,1	10	58,9	3,11
439401-1485	97001-47	16	31,6	24,1	3,4	72,4	7,09
439401-1545	97001-18	16	24	8,3	5,6	86,1	1,48
439401-1725	97001-19	10	35,1	8	4	88	2,00
439401-1830	97001-56	5	45,2	7,5	5	87,5	1,50
439401-2145	97001-64	3	34,4	43,8	12,5	43,8	3,50
439401-2300	97001-72	1	35,7	21,4	14,3	64,3	1,50
439401-2510	97001-79B			0	50	50	0,00
439401-2510	97001-79	3	20	15,4	7,7	76,9	2,00
439401-2875	97001-89	2	30,8	33,3	16,7	50	1,99
439401-2950	97001-91			16,7	0	83,3	n.a.

Table 3

Gas Chormatography data

Sample	pr/ph	pr/nC17	ph/nC18	iso/nC	CPI	Philippi
439401-320	6,45	1,95	0,27	0,52	1,30	1,84
439401-330	7,47	3,08	0,39	0,85	1,26	1,68
439401-340	4,55	0,81	0,16	0,23	1,20	1,50
439401-350	5,98	4,18	0,70	1,15	1,31	1,79
439401-360	7,48	5,70	0,80	1,58	1,27	1,65
439401-370	6,25	2,60	0,35	0,61	1,10	0,18
439401-380	6,81	3,81	0,57	1,06	1,27	1,73
439401-390	5,72	2,09	0,31	0,53	1,21	1,58
439401-400	5,75	2,40	0,40	0,68	1,26	1,66
439401-410	6,15	2,07	0,31	0,67	1,22	1,60
439401-420	6,72	2,39	0,40	0,75	1,22	1,54
439401-430	5,96	2,78	0,47	0,81	1,24	1,64
439401-440	5,77	4,06	0,70	1,11	1,29	1,72
439401-510	4,31	1,49	0,33	0,44	1,31	1,95
439401-990	4,48	1,00	0,20	0,28	1,13	1,32
439401-1150	4,29	0,82	0,18	0,27	1,12	1,29
439401-1170	4,45	0,68	0,14	0,22	1,08	1,22
439401-1180	4,33	0,72	0,15	0,22	1,09	1,27
439401-1230	4,86	0,68	0,14	0,23	1,06	1,18
439401-1250	4,71	0,37	0,08	0,14	1,05	1,15
439401-1370	4,17	0,51	0,13	0,19	1,09	1,29
439401-1440	4,05	0,64	0,16	0,24	1,06	1,16
439401-1485	4,96	0,44	0,09	0,16	1,05	1,19
439401-1545	3,89	0,84	0,23	0,30	1,09	1,47
439401-1725	1,05	0,39	0,38	0,27	1,19	1,50
439401-1830	1,31	0,45	0,35	0,24	1,02	1,38
439401-2145	1,14	0,56	0,37	0,23	1,08	1,29
439401-2300	0,99	0,49	0,41	0,27	0,98	1,39
439401-2510	n.a.	n.a	n.a.	n.a.	n.a.	n.a.
439401-2510	0,91	0,42	0,41	0,21	2,00	3,01
439401-2875	0,65	0,35	0,41	0,23	1,11	1,57
439401-2950	1,18	0,51	0,61	0,34	1,50	1,97

pr/ph: pristane/phytane ratio
pr/nC17: pristane/heptadecane ratio
pr/nC18: phytane/octadecane ratio
Iso/nC: $C_{15\text{-}20}$ isoprenoid/$C_{15\text{-}20}$ n-alkane ratio
CPI: Carbon Preference Indeks
Philippi: $(2*nC_{29})/(nC_{28}+nC_{30})$

Table 4

Triterpanes, m/z 191

	T23/H30	TE24/H30	BNL/H30	H29/H30	O+L/H30	HOEP
439401-320	0,01	0,07	0,38	0,91	0,20	1,32
439401-330	0,01	0,07	0,30	0,85	0,08	1,18
439401-340	0,01	0,06	0,33	0,66	0,45	1,09
439401-350	0,01	0,07	0,38	0,91	0,11	1,15
439401-360	0,02	0,10	0,40	0,91	0,13	1,18
439401-370	0,01	0,07	0,41	0,80	0,11	1,10
439401-380	0,02	0,10	0,46	1,05	0,03	1,16
439401-390	0,03	0,10	0,48	1,06	0,11	1,14
439401-400	0,03	0,09	0,31	1,06	0,07	1,11
439401-410	0,02	0,09	0,35	1,07	0,18	1,10
439401-420	0,02	0,09	0,30	1,00	0,08	1,08
439401-430	0,02	0,09	0,28	0,91	0,08	1,10
439401-440	0,01	0,08	0,22	0,85	0,02	1,16
439401-510	0,01	0,04	0,13	0,75	0,06	1,04
439401-990	0,03	0,14	0,06	0,42	0,53	0,95
439401-1150	0,05	0,21	0,07	0,41	0,40	0,85
439401-1170	0,10	0,24	0,13	0,37	0,43	0,85
439401-1180	0,10	0,20	0,09	0,43	0,35	0,88
439401-1230	0,17	0,20	0,13	0,59	0,43	1,00
439401-1250	0,52	0,30	0,15	0,63	1,19	0,96
439401-1370	0,44	0,17	0,24	0,73	0,35	1,08
439401-1440	0,30	0,23	0,08	0,53	0,49	0,95
439401-1485	0,77	0,23	0,00	0,88	0,91	0,38
439401-1545	1,96	0,45	0,00	0,90	0,23	1,10
439401-1725	0,75	0,31	0,00	0,62	0,06	1,01
439401-1830	0,69	0,21	0,00	0,67	0,05	1,03
439401-2145	0,43	0,09	0,00	0,55	0,05	1,15
439401-2300	0,22	0,10	0,00	0,39	0,05	1,21
439401-2510	n.a.	n.a.	n.a.	n.a.	n.a.	n.a.
439401-2510	n.a.	n.a.	n.a.	n.a.	n.a.	n.a.
439401-2875	1,72	0,27	0,00	0,72	0,00	1,17
439401-2950	n.a.	n.a.	n.a.	n.a.	n.a.	n.a.

T23/H30 = C_{23} tricyclic triterpane to C_{30} hopane ratio
T24/H30 = C_{24} tetracyclic terpane to C_{30} hopane ratio
BNL/H30 = bisnorlupane/hopane
H29/H30 = norhopane to hopane ratio
O+L/H30 = oleanane+lupane/hopane
HOEP = Homohopane odd/even predominance

Table 5

Steranes, m/z 217

	D27/S27	S27 (%)	S28 (%)	S29 (%)	S27/S29	S30
439401-320	0,44	10,9	13,6	75,5	0,1	absent
439401-330	0,52	14,0	10,8	75,3	0,2	absent
439401-340	0,47	21,8	13,3	64,9	0,3	absent
439401-350	0,46	10,7	10,7	78,7	0,1	absent
439401-360	0,53	14,3	12,9	72,9	0,2	absent
439401-370	0,58	18,7	13,3	68,0	0,3	absent
439401-380	0,47	15,6	12,2	72,2	0,2	absent
439401-390	0,56	17,6	13,3	69,1	0,3	absent
439401-400	0,60	16,0	16,6	67,5	0,2	absent
439401-410	0,59	15,8	16,4	67,8	0,2	absent
439401-420	0,59	16,0	16,8	67,2	0,2	absent
439401-430	0,64	16,0	17,6	66,4	0,2	absent
439401-440	0,57	12,8	20,8	66,4	0,2	absent
439401-510	0,56	14,6	12,1	73,4	0,2	absent
439401-990	0,71	11,8	32,6	55,6	0,2	absent
439401-1150	0,65	20,5	32,5	47,0	0,4	absent
439401-1170	0,72	27,2	32,0	40,8	0,7	absent
439401-1180	0,64	21,7	30,4	47,8	0,5	absent
439401-1230	0,90	25,8	25,8	48,4	0,5	absent
439401-1250	1,04	27,4	30,8	41,9	0,7	absent
439401-1370	1,04	33,8	25,7	40,5	0,8	absent
439401-1440	1,06	31,1	25,8	43,2	0,7	absent
439401-1485	n.a.	21,5	21,5	57,0	0,4	absent
439401-1545	1,29	41,7	26,2	32,1	1,3	present
439401-1725	1,07	41,3	17,5	41,3	1,0	present
439401-1830	0,95	48,5	17,8	33,7	1,4	present
439401-2145	0,76	30,2	23,3	46,5	0,6	present
439401-2300	0,96	42,7	18,5	38,9	1,1	present
439401-2510	n.a.	n.a.	n.a.	n.a.	n.a.	absent
439401-2510	n.a.	n.a.	n.a.	n.a.	n.a.	absent
439401-2875	0,87	38,9	17,1	44,0	0,9	present
439401-2950	0,94	26,5	13,2	60,3	0,4	absent

D27/S27 = Ratio of C_{27} diasteranes to C_{27} regular steranes
S27 (%), S28 (%), S29)(%) = Relative distribution of C_{27-29} regular steranes based on aaaR isomers in m/z
S27/S29 = Ratio of C_{27} to C_{29} regular steranes
S30 = C_{30} steranes

Table 6

Thermal maturity indicators

	S29 S/(S+R)	S29 ββ/(ββ+αα)	H31 S/(S+R)	H32 S/(S+R)	Ts/(Ts+Tm)	Tm/Tm+17β
439401-320	0,42	0,32	0,59	0,59	0,09	1,00
439401-330	0,52	0,31	0,58	0,59	0,09	1,00
439401-340	0,43	0,33	0,59	0,58	0,14	1,00
439401-350	0,51	0,37	0,59	0,61	0,07	1,00
439401-360	0,60	0,33	0,60	0,60	0,07	1,00
439401-370	0,62	0,28	0,60	0,63	0,07	1,00
439401-380	0,51	0,45	0,59	0,58	0,06	1,00
439401-390	0,53	0,44	0,60	0,60	0,06	1,00
439401-400	0,52	0,34	0,59	0,60	0,06	1,00
439401-410	0,51	0,32	0,58	0,59	0,07	1,00
439401-420	0,53	0,35	0,60	0,59	0,07	1,00
439401-430	0,53	0,34	0,58	0,57	0,09	1,00
439401-440	0,51	0,42	0,60	0,61	0,11	1,00
439401-510	0,36	0,34	0,57	0,60	0,18	1,00
439401-990	0,49	0,57	0,57	0,62	0,42	1,00
439401-1150	0,50	0,54	0,59	0,60	0,64	1,00
439401-1170	0,49	0,58	0,59	0,61	0,74	1,00
439401-1180	0,47	0,56	0,54	0,64	0,67	1,00
439401-1230	0,45	0,55	0,57	0,59	0,79	1,00
439401-1250	0,48	0,61	0,53	0,65	0,76	1,00
439401-1370	0,53	0,53	0,47	0,62	0,64	1,00
439401-1440	0,47	0,56	0,59	0,61	0,70	1,00
439401-1485	0,51	0,58	0,53	0,55	0,67	1,00
439401-1545	0,52	0,54	0,50	0,60	0,53	1,00
439401-1725	0,46	0,57	0,56	0,62	0,47	1,00
439401-1830	0,44	0,55	0,60	0,59	0,53	1,00
439401-2145	0,42	0,58	0,52	0,59	0,57	1,00
439401-2300	0,43	0,53	0,60	0,58	0,43	1,00
439401-2510	n.a.	n.a.	n.a	n.a	n.a.	n.a.
439401-2510	n.a.	n.a.	n.a	n.a	n.a.	n.a.
439401-2875	0,37	0,59	0,36	0,58	0,52	1,00
439401-2950	0,33	0,30	n.a	n.a	n.a.	n.a.

S29 S/(S+R) = C_{29} sterane 20S/(20S+20R)
S29 ββ(/ββ+αα) = C_{29} sterane αββ/(αββ+ααα)
H31 S/(S+R) = homohopane 22S/(22S+22R)
H32 S/(S+R) = bishomohopane 22S/(22S+22R)

Table 7